Weak Lensing and Cosmology

Martin Kilbinger

Institut d'Astrophysique de Paris

IPM Cosmology School and Workshop 2007, Tehran
June 2 – 9 2007

Overview

Lensing by the large-scale structure

- (Weak) gravitational lensing in a nutshell
- Deflection in an inhomogeneous Universe
- Shear and convergence
- Projected power spectrum and cosmological parameters

Weak lensing and cosmology

- Second-order cosmic shear statistics
- Shear tomography (2 1/2 D lensing)
- Third-order cosmic shear statistics
- 3D lensing
- Peak statistics
- Shear-ratio geometry test

Observational aspects of weak lensing

- Shape measurement
- Photometric redshifts
- Intrinsic alignment
- Non-linear structure formation
- Non-Gaussian errors

Books & Reviews

- Kochanek, Schneider & Wambsganss, Gravitational lensing: Strong, weak & micro, proceedings of the 33rd Saas-Fee Advanced Course, 2004, Springer (http://www.astro.uni-bonn.de/~peter/SaasFee.html)
- Bartelmann & Schneider, Weak gravitational lensing, 2001, Phys. Rep. , 340, 297 (astro-ph/9912508)
- Refregier, Weak gravitational lensing by large-scale structure, 2003, ARA&A, 41, 645 (astro-ph/0307212)
- van Waerbeke & Mellier, Gravitational lensing by large scale structures: A review, Aussois winter school, astro-ph/0305089)
- Munshi et al. 2007, Cosmology with weak lensing surveys, submitted to Phys.Rep., astro-ph/0612667

Lensing by the large-scale structure

Overview

- (Weak) gravitational lensing in a nutshell
- Deflection of light in an inhomogeneous Universe
- Shear γ and convergence κ
- Projected power spectrum and cosmological parameters

(Weak) gravitational lensing in a nutshell

Gravitational lensing theory

Phenomenon of gravitational light deflection in the limits of weak, stationary fields and small deflection angles

Basis is General Theory of Relativity

Photons travel on null geodesics of space-time metric. Simplified mathematical treatment of GL.

Achievements of weak lensing

Cluster masses, mass profiles, M/L-relation, SI cross-section of dark matter, galaxy halos at large scales, power spectrum normalization σ_8, Ω_m, structure growth

Probing matter distribution using distant galaxies

- Light from distant galaxies is continuously deflected on its way through an inhomogeneous Universe
- Light bundles are differentially distorted due to gravitational lensing by tidal field of large-scale structure (LSS)

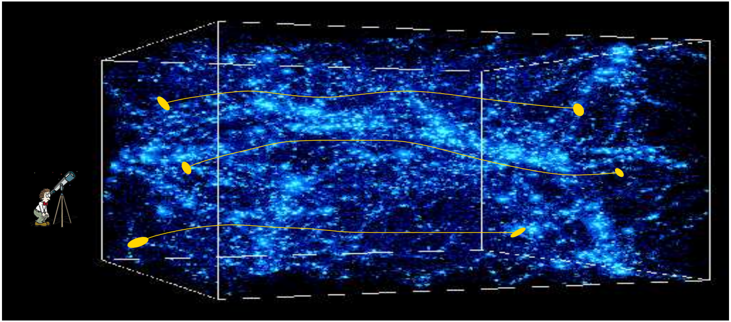

- Images of galaxies are coherently distorted leading to shape correlations which depend on statistical properties of LSS
- Probes total (dark+luminous) matter, no tracer for dark matter needed
- Distortions are very small (weak lensing regime), can be detected only statistically using large number of galaxies

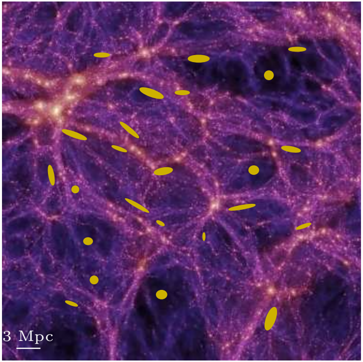

"Cosmic shear"

Deflection angle

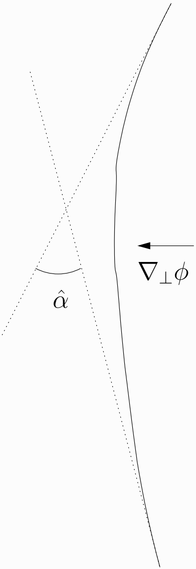

- Perturbed Minkowski metric, weak field $\phi \ll c^2$

$$\mathrm{d}s^2 = \left(1 + 2\phi/c^2\right) c^2 \mathrm{d}t^2 - \left(1 - 2\phi/c^2\right) \mathrm{d}\ell^2$$

- Fermat's principle: light travel time stationary

$$t = \frac{1}{c} \int_{\mathrm{path}} \left(1 - 2\phi/c^2\right) \mathrm{d}\ell$$

- Deflection angle

$$\boldsymbol{\alpha} = -\frac{2}{c^2} \int_{\mathrm{S}}^{\mathrm{O}} \boldsymbol{\nabla}_\perp \phi \, \mathrm{d}\ell$$

Propagation of light bundles

- Comoving separation $\boldsymbol{x}$ between two light rays from geodesic deviation equation, relating neighboring geodesics via Riemann tensor

$$\longrightarrow \frac{\mathrm{d}^2\boldsymbol{x}}{\mathrm{d}w^2} + K\boldsymbol{x} = -\frac{2}{c^2}\Delta\Big(\nabla_\perp\phi(\boldsymbol{x}, w)\Big).$$

(w = comoving distance, K = spatial curvature)

- Solution is integral equation

$$\boldsymbol{x}(\boldsymbol{\theta}, w) = f_K(w)\boldsymbol{\theta} - \frac{2}{c^2}\int_0^w dw' f_K(w-w')\Delta\Big(\nabla_\perp\phi(\boldsymbol{x}(\boldsymbol{\theta}, w'), w')\Big).$$

($f_K(w)$ = comoving angular diameter distance)

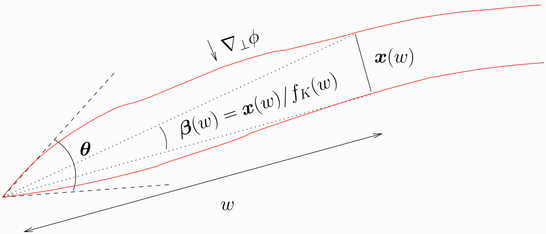

Deflection angle

Solving differential equation

- Born approximation: replace $\boldsymbol{x}$ on r.h.s. with $\boldsymbol{x}_0(\boldsymbol{\theta}, w) = f_K(w)\,\boldsymbol{\theta}$ (integrate along unperturbed ray)
- Deflection angle = difference between angular separation of two light rays in unperturbed and perturbed Universe, at comoving distance w

$$\begin{aligned}\boldsymbol{\alpha}(\boldsymbol{\theta}, w) \equiv \boldsymbol{\theta} - \boldsymbol{\beta}(\boldsymbol{\theta}, w) &= \frac{f_K(w)\boldsymbol{\theta} - \boldsymbol{x}(\boldsymbol{\theta}, w)}{f_K(w)} \\ &= \frac{2}{c^2}\int_0^w \mathrm{d}w' \, \frac{f_K(w-w')}{f_K(w)} \nabla_\perp \phi[f_K(w')\boldsymbol{\theta}, w'), w']\end{aligned}$$

- Lensing potential, $\boldsymbol{\alpha} = \nabla\psi$

$$\psi(\boldsymbol{\theta}, w) = \frac{2}{c^2}\int_0^w \mathrm{d}w' \, \frac{f_K(w-w')}{f_K(w')f_K(w)} \phi(f_K(w')\boldsymbol{\theta}, w')$$

Linearizing the lens mapping

- $\boldsymbol{\beta}(\boldsymbol{\theta}) = \boldsymbol{\theta} - \boldsymbol{\alpha}(\boldsymbol{\theta})$ is mapping from unperturbed ($\boldsymbol{\theta}$) to unperturbed ($\boldsymbol{\beta}$) coordinates (lens equation)
- Linearize mapping, defining Jacobian

$$\mathcal{A}_{ij} = \frac{\partial \beta_i}{\partial \theta_j} == \delta_{ij} - \frac{\partial^2 \psi}{\partial \theta_i \partial \theta_j} = \begin{pmatrix} 1-\kappa-\gamma_1 & -\gamma_2 \\ -\gamma_2 & 1-\kappa+\gamma_1 \end{pmatrix}$$

defining convergence κ and shear γ as second-order derivatives of lensing potential

$$\kappa = \frac{1}{2}(\partial_1\partial_1 + \partial_2\partial_2)\psi$$

$$\gamma_1 = \frac{1}{2}\left(\partial_1\partial_1 - \partial_2\partial_2\right)\psi; \qquad \gamma_2 = \partial_1\partial_2\psi$$

- Reduced shear $g_i = \gamma_i/(1-\kappa)$

Shear and convergence

Liouville's theorem: Surface brightness is conserved

$$I(\boldsymbol{\theta}) = I^{\mathrm{s}}(\boldsymbol{\beta}(\boldsymbol{\theta})) \approx I^{\mathrm{s}}(\boldsymbol{\beta}(\boldsymbol{\theta}_0) + \mathcal{A}(\boldsymbol{\theta} - \boldsymbol{\theta}_0))$$

Effect of lensing

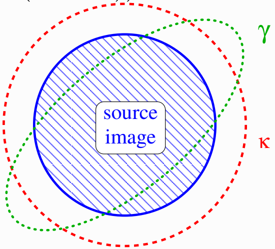

- isotropic magnification (convergence κ)
- anisotropic stretching (shear γ)

Shear transforms a circle into an ellipse.
Define complex ellipticity

$$\gamma = \gamma_1 + \mathrm{i}\gamma_2 = |\gamma|\mathrm{e}^{2\mathrm{i}\varphi};$$

$$|\gamma| = |1-\kappa|\frac{1-b/a}{1+b/a}$$

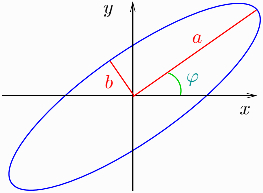

Basic equation of weak lensing

Weak lensing regime

$\kappa \ll 1, |\gamma| \ll 1.$

The observed ellipticity of a galaxy is the sum of the intrinsic ellipticity and the shear:

$$\boxed{\varepsilon \approx \varepsilon^{\mathrm{s}} + \gamma}$$

Random intrinsic orientation of galaxies

$$\langle \varepsilon^{\mathrm{s}} \rangle = 0 \quad \longrightarrow \quad \boxed{\langle \varepsilon \rangle = \gamma}$$

The observed ellipticity is an unbiased estimator of the shear. Very noisy though! $\sigma_\varepsilon = \langle |\varepsilon^{\mathrm{s}}|^2 \rangle^{1/2} \approx 0.3 - 0.4 \gg \gamma$. Beat down noise by averaging over large number of galaxies.

Ellipticity and local shear

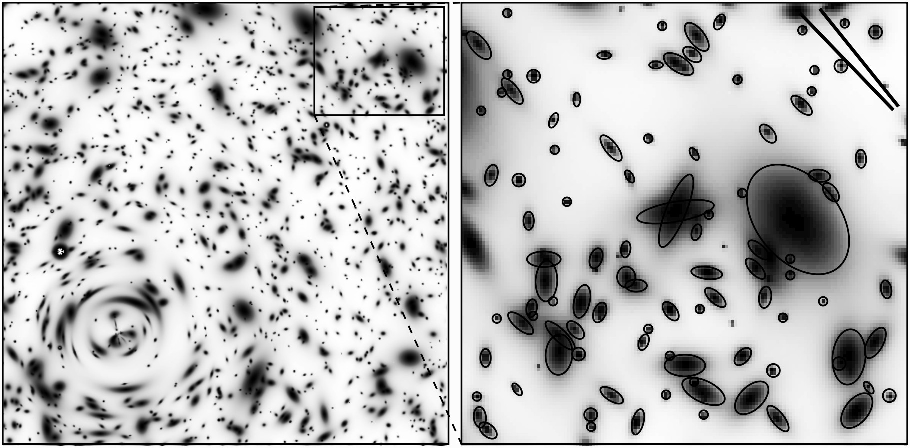

[from Y. Mellier]

Galaxy ellipticities are an estimator of the local shear.

Typical numbers

Regime	γ	$\gamma/\sigma_\varepsilon$	$N_{\rm gal}$ for S/N~ 1
weak lensing by clusters	0.03	0.1	10^2
galaxy-galaxy lensing	0.003	0.01	10^4
cosmic shear	0.001	0.003	10^5

Much more galaxies for precision measurements needed.

Cosmic shear galaxy surveys

$n_{\rm gal}$ [arcmin^{-2}]	10 – 30	(from ground)
	60 – 100	(from space)

Area:
- past: from < 1 deg^2 to ≈ 100 deg^2.
- ongoing: Subaru (33 deg^2), DLS (36 deg^2), CFHTLS-Wide (170 deg^2)
- future: DES, KIDS, SNAP (1000–5000 deg^2), Pan-STARRS-4, LSST, DUNE (20 000 deg^2)

Relation to density contrast

Back to the propagation equation

- Since $\kappa = \frac{1}{2}\Delta\psi$:

$$\kappa(\boldsymbol{\theta}, w) = \frac{1}{c^2} \int_0^w \mathrm{d}w' \frac{f_K(w-w') f_K(w')}{f_K(w)} \Delta_{\boldsymbol{\theta}} \Phi(f_K(w')\boldsymbol{\theta}, w')$$

- Terms $\Delta_{w'w'}\Phi$ average out when integrating along line of sight, can be added to yield 3d Laplacian (error $\mathcal{O}(\Phi) \sim 10^{-5}$).
- Poisson equation

$$\Delta\Phi = \frac{3H_0^2\Omega_\mathrm{m}}{2a}\,\delta$$

$$\rightarrow \kappa(\boldsymbol{\theta}, w) = \frac{3}{2}\Omega_\mathrm{m} \left(\frac{H_0}{c}\right)^2 \int_0^w \mathrm{d}w' \frac{f_K(w-w') f_K(w')}{f_K(w) a(w')}\, \delta\left(f_K(w')\boldsymbol{\theta}, w'\right).$$

Amplitude of the cosmic shear signal

Order-of magnitude estimate

$$\kappa(\boldsymbol{\theta}, w) = \frac{3}{2}\Omega_{\mathrm{m}} \left(\frac{H_0}{c}\right)^2 \int_0^w \mathrm{d}w' \frac{f_K(w-w') f_K(w')}{f_K(w) a(w')} \, \delta\left(f_K(w')\boldsymbol{\theta}, w'\right).$$

for simple case: single lens at at redshift $z_{\mathrm{L}} = 0.4$ with size R, source at $z_{\mathrm{S}} = 0.8$.

$$\kappa \approx \frac{3}{2}\Omega_{\mathrm{m}} \left(\frac{H_0}{c}\right)^2 \frac{D_{\mathrm{LS}} D_{\mathrm{L}}}{D_{\mathrm{S}}} \frac{R}{a^2(z_{\mathrm{L}})} \frac{\delta\rho}{\rho}$$

Add signal from $N \approx D_{\mathrm{S}}/R$ crossings:

$$\begin{aligned} \langle \kappa^2 \rangle^{1/2} \approx & \frac{3}{2}\Omega_{\mathrm{m}} \frac{D_{\mathrm{LS}} D_{\mathrm{L}}}{R_{\mathrm{H}}^2} \sqrt{\frac{R}{D_{\mathrm{S}}}} a^{-1.5}(z_{\mathrm{L}}) \left\langle \left(\frac{\delta\rho}{\rho}\right)^2 \right\rangle \\ \approx & \frac{3}{2} \, 0.3 \times 0.1 \quad \times \; 0.1 \quad \times 2 \qquad\quad \times 1 \qquad\quad \approx 0.01 \end{aligned}$$

- Convergence signal from a distribution of source galaxies with pdf $p(w)\mathrm{d}w$

$$\kappa(\boldsymbol{\theta}) = \int_0^{w_{\mathrm{lim}}} \mathrm{d}w\, p(w)\, \kappa(\boldsymbol{\theta}, w) = \int_0^{w_{\mathrm{lim}}} \mathrm{d}w\, G(w)\, f_K(w)\, \delta\left(f_K(w)\boldsymbol{\theta}, w\right)$$

with lens efficiency

$$G(w) = \frac{3}{2}\left(\frac{H_0}{c}\right)^2 \frac{\Omega_{\mathrm{m}}}{a(w)} \int_w^{w_{\mathrm{lim}}} \mathrm{d}w'\, p(w') \frac{f_K(w'-w)}{f_K(w')}.$$

The convergence is a projection of the matter-density contrast, weighted by the source galaxy distribution and angular distances.

Parametrization of redshift distribution, e.g.

$$p(w)\mathrm{d}w = p(z)\mathrm{d}z \propto (z/z0)^{\alpha} \exp[-(z/z0)^{\beta}]$$

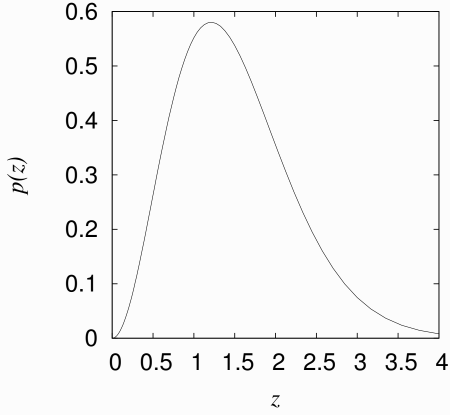

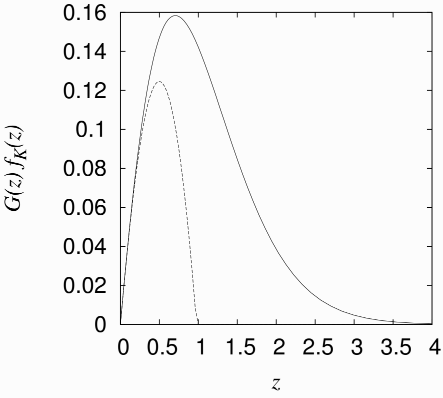

$\alpha = 2, \beta = 1.5, z_0 = 1$

dashed line: all sources at redshift 1

The convergence power spectrum

- Variance of convergence $\langle \kappa(\boldsymbol{\vartheta} + \boldsymbol{\theta}) \kappa(\boldsymbol{\vartheta}) \rangle = \langle \kappa\kappa \rangle(\theta)$ depends on variance of the density contrast $\langle \delta\delta \rangle$
- In Fourier space:

$$\left\langle \hat{\kappa}(\boldsymbol{\ell}) \hat{\kappa}^*(\boldsymbol{\ell}') \right\rangle = (2\pi)^2 \delta_{\mathrm{D}}(\boldsymbol{\ell} - \boldsymbol{\ell}') P_\kappa(\ell)$$
$$\left\langle \hat{\delta}(\boldsymbol{k}) \hat{\delta}^*(\boldsymbol{k}') \right\rangle = (2\pi)^3 \delta_{\mathrm{D}}(\boldsymbol{k} - \boldsymbol{k}') P_\delta(k)$$

- Limber's equation

$$P_\kappa(\ell) = \int \mathrm{d}w \, G^2(w) P_\delta \left(\frac{\ell}{f_K(w)} \right)$$

using small-angle approximation, $P_\delta(k) \approx P_\delta(k_\perp)$, contribution only from Fourier modes $\perp$ to line of sight

- Relations between κ and γ $\longrightarrow$ $\boxed{P_\kappa = P_\gamma}$

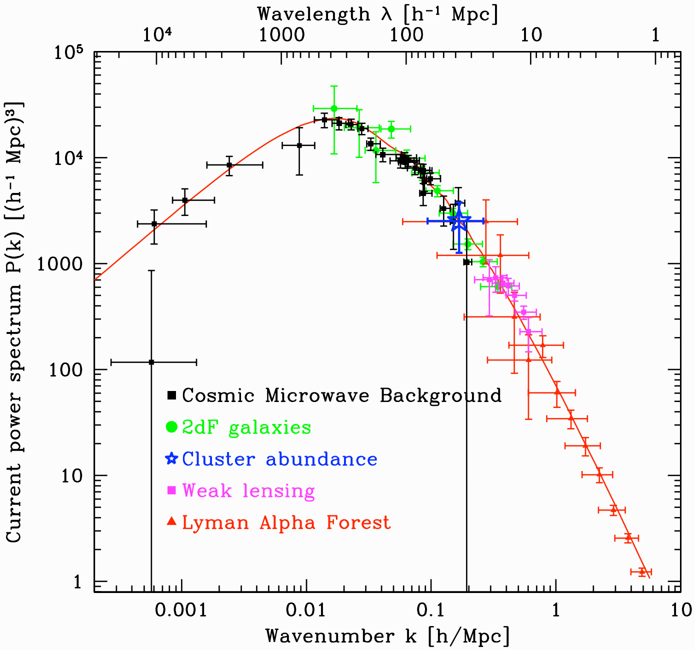

Wavelength λ [h⁻¹ Mpc]
10⁴
1000
100
10
1
10⁵
10⁴
1000
100
10
1
Current power spectrum P(k) [(h⁻¹ Mpc)³]
Cosmic Microwave Background
2dF galaxies
Cluster abundance
Weak lensing
Lyman Alpha Forest
0.001
0.01
0.1
1
10
Wavenumber k [h/Mpc]

[M. Tegmark]

Convergence power spectrum

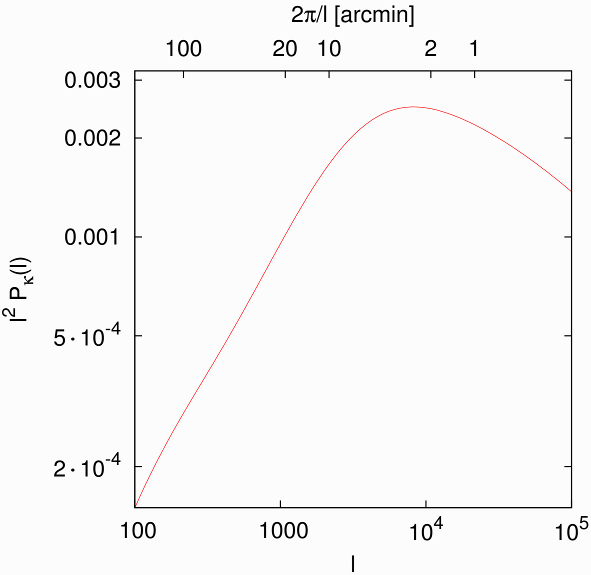

Example

A simple toy model: single lens plane at redshift z_0, $P_\delta(k) \propto \sigma_8^2 k^n$, CDM, no Λ, linear growth:

$$\langle \kappa^2(\theta) \rangle^{1/2} = \langle \gamma^2(\theta) \rangle^{1/2} \approx 0.01\, \sigma_8\, \Omega_{\rm m}^{0.8} \left(\frac{\theta}{1 \mathrm{deg}} \right)^{-(n+2)/2} z_0^{0.75}$$

Born-approximation tested with numerical (ray-tracing) simulations.

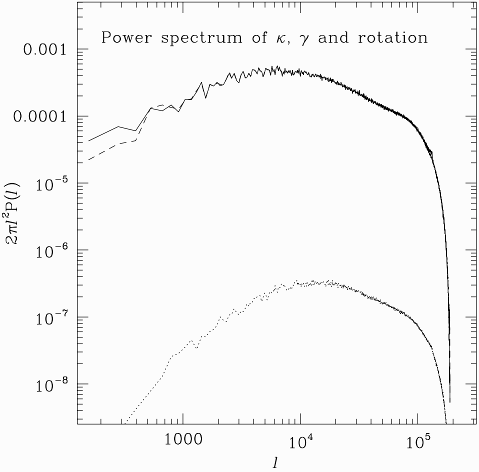

Asymmetry of Jacobi-matrix $\mathcal{A}$ due to lens-lens coupling negligible
[Jain, Seljak & White 2000]

Cosmic shear and cosmology

Overview

- Second-order cosmic shear statistics
- Shear tomography (2 1/2 D lensing)
- Third-order cosmic shear statistics
- 3D lensing
- Peak statistics
- Shear-ratio geometry test
- (Flexion)

Shear components

- Recall: complex shear $\gamma = \gamma_1 + \mathrm{i}\gamma_2 = |\gamma| \exp(2\mathrm{i}\phi)$ is measure of an object's ellipticity
- Tangential and cross-component

$$\gamma_{\mathrm{t}} = -\Re\left(\gamma \mathrm{e}^{-2\mathrm{i}\varphi}\right) \qquad \text{and} \qquad \gamma_{\times} = -\Im\left(\gamma \mathrm{e}^{-2\mathrm{i}\varphi}\right)$$

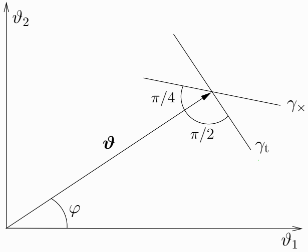

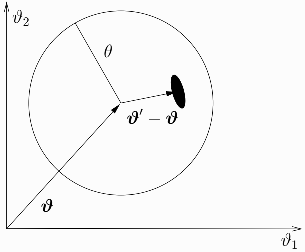

Shear is polar/Spin-2 quantity!

Shear in apertures

- Aperture mass: weighted convergence/shear in a circle

$$M_{\mathrm{ap}}(\theta) = \int \mathrm{d}^2\vartheta' \, U_\theta(\vartheta') \kappa(\boldsymbol{\vartheta}') = \int \mathrm{d}^2\vartheta' \, Q_\theta(\vartheta') \gamma_{\mathrm{t}}(\boldsymbol{\vartheta}'),$$

  U_θ is a compensated filter

$$\int \mathrm{d}\vartheta \, \vartheta \, U_\theta(\vartheta) = 0$$

- Filter functions are related

$$Q_\theta(\vartheta) = \frac{2}{\vartheta^2} \int_0^\vartheta \mathrm{d}\vartheta' \, \vartheta' \, U_\theta(\vartheta') - U_\theta(\vartheta).$$

Convergence and shear field

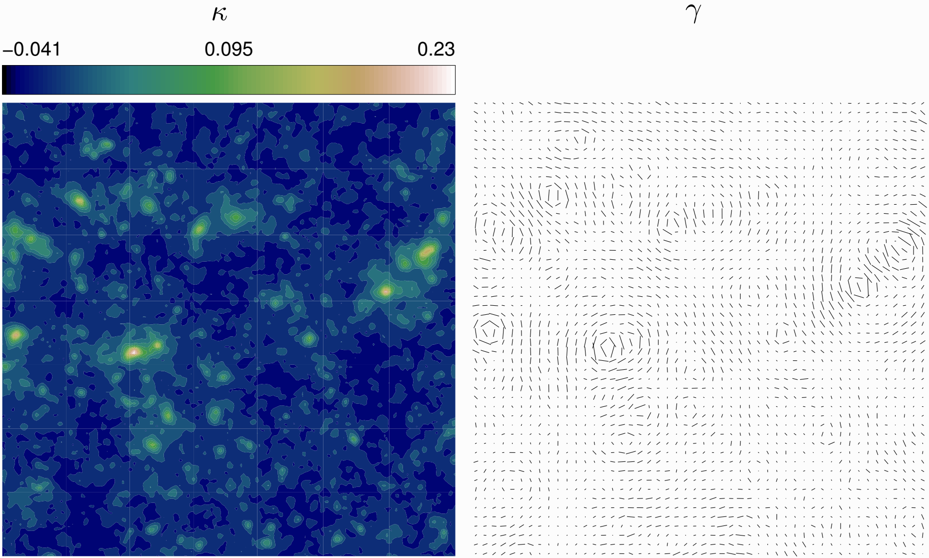

N-body simulation and ray-tracing from T.Hamana

Aperture filter functions

	polynomial	Gaussian
$U_\theta(\vartheta)$	$\begin{cases} \frac{9}{\pi\theta^2}\left(1-\frac{\vartheta^2}{\theta^2}\right)\left(\frac{1}{3}-\frac{\vartheta^2}{\theta^2}\right) & \lvert\vartheta\rvert<\theta \\ 0 & \text{else} \end{cases}$	$\frac{1}{2\pi\theta^2}\left(1-\frac{\vartheta^2}{2\theta^2}\right)\exp\left(-\frac{\vartheta^2}{2\theta^2}\right)$
$Q_\theta(\vartheta)$	$\begin{cases} \frac{6}{\pi\theta^2}\frac{\vartheta^2}{\theta^2}\left(1-\frac{\vartheta^2}{\theta^2}\right) & \lvert\vartheta\rvert<\theta \\ 0 & \text{else} \end{cases}$	$\frac{\vartheta^2}{4\pi\theta^4}\exp\left(-\frac{\vartheta^2}{2\theta^2}\right)$
$\hat{U}(\eta)$	$\frac{24\mathrm{J}_4(\eta)}{\eta^2}$	$\frac{\eta^2}{2}\exp\left(\frac{-\eta^2}{2}\right)$

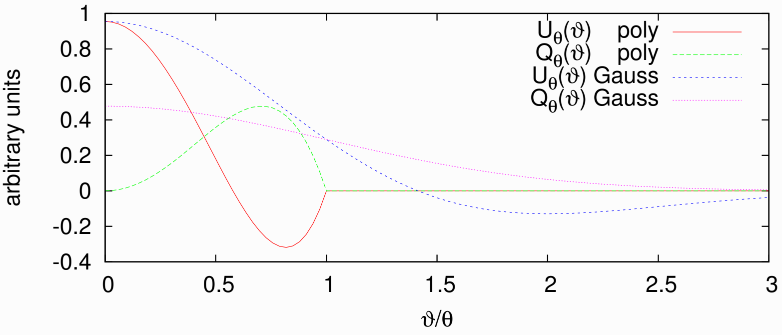

Second-order statistics

- Correlation of the shear at two points yields four quantities

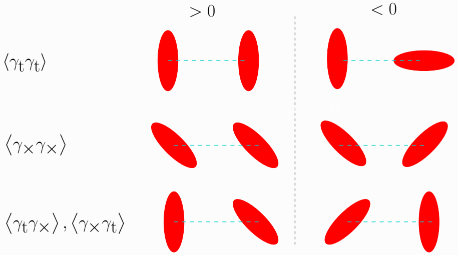

- Parity conservation $\longrightarrow \langle\gamma_t\gamma_\times\rangle = \langle\gamma_\times\gamma_t\rangle = 0$
- Shear two-point correlation function (2PCF)

$$\xi_+(\vartheta) = \langle\gamma_t\gamma_t\rangle(\vartheta) + \langle\gamma_\times\gamma_\times\rangle(\vartheta)$$
$$\xi_-(\vartheta) = \langle\gamma_t\gamma_t\rangle(\vartheta) - \langle\gamma_\times\gamma_\times\rangle(\vartheta)$$

Relation to the power spectrum

- Two-point correlation function

$$\xi_+(\theta) = \frac{1}{2\pi} \int \mathrm{d}\ell \, \ell \mathrm{J}_0(\ell\theta) P_\kappa(\ell)$$
$$\xi_-(\theta) = \frac{1}{2\pi} \int \mathrm{d}\ell \, \ell \mathrm{J}_4(\ell\theta) P_\kappa(\ell),$$

- Aperture-mass variance/dispersion

$$\langle M_{\mathrm{ap}}^2 \rangle(\theta) = \frac{1}{2\pi} \int \mathrm{d}\ell \, \ell \, P_\kappa(\ell) \hat{U}^2(\theta\ell)$$

- Top-hat-variance

$$\langle |\bar{\gamma}|^2 \rangle(\theta) = \frac{1}{\pi\theta^2} \int \mathrm{d}^2\vartheta \, \gamma(\boldsymbol{\vartheta}) \gamma^*(\boldsymbol{\vartheta})$$
$$= \frac{1}{2\pi} \int \mathrm{d}\ell \, \ell \, P_\kappa(\ell) \left[\frac{2\mathrm{J}_1(\ell\theta)}{\ell\theta} \right]^2$$

Filter functions

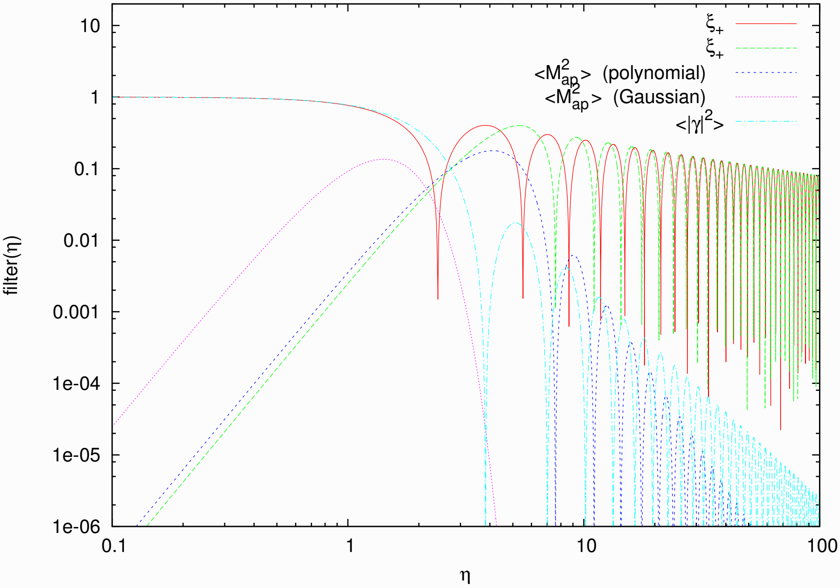

Second-order shear statistics

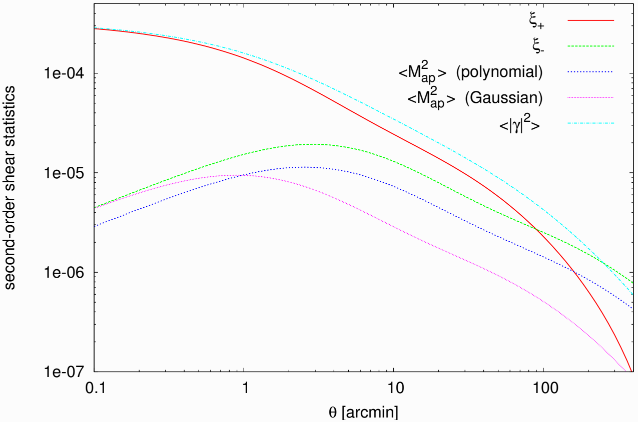

- $\langle M_{\rm ap}^2\rangle$ is narrow band-pass filter of $P_\kappa \longrightarrow$ localized probe
- ξ_+, $\langle|\bar\gamma|^2\rangle$ are low-pass filter of $P_\kappa \longrightarrow$ high S/N, sensitive to large scales

Dependence on cosmology

growth of structures,
initial conditions

$$P_\kappa(\ell) = \int \mathrm{d}w \, G^2(w) P_\delta\left(\frac{\ell}{f_K(w)}\right)$$

$$G(w) = \frac{3}{2}\left(\frac{H_0}{c}\right)^2 \frac{\Omega_\mathrm{m}}{a(w)} \int_w^{w_\mathrm{lim}} \mathrm{d}w' \, p(w') \frac{f_K(w'-w)}{f_K(w')}$$

cosmological
Parameters

redshift distribution
of source galaxies

geometrical factors

Parameter degeneracies

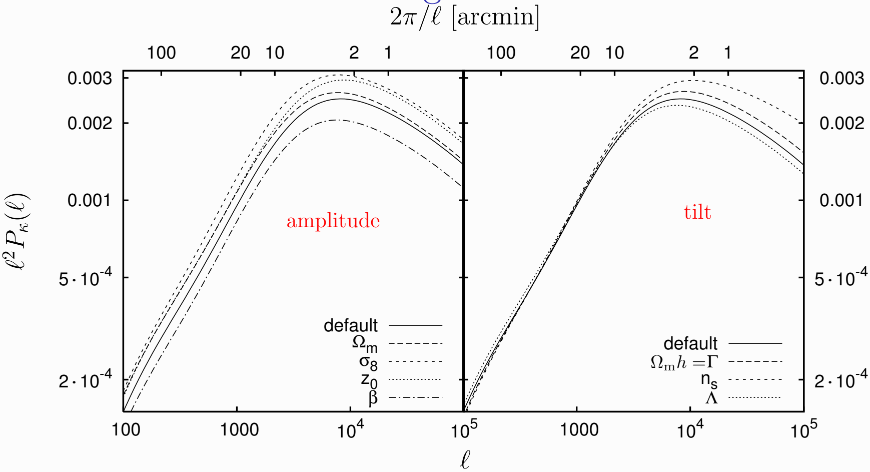

Cosmological parameters from weak lensing show high level of near-degeneracies. P_κ relatively featureless because of projection and non-linear growth.

Cosmology from cosmic shear

- Probes Universe at low – medium redshifts ($z \sim 0.2 - 0.8$). That's where dark energy is important!
- Probes LSS at small scales ($R \sim 0.3h^{-1}(\theta/1')$ Mpc): non-linear & non-Gaussian structure formation
- Independent of relation between dark & luminous matter (e.g. galaxy bias)
- Most sensitive to Ω_{m} and power spectrum normalization σ_8
- Complementary & independent method

$\Omega_m - \sigma_8$

CFHTLS Wide

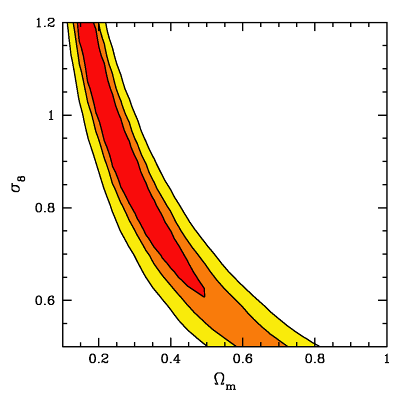

$\sigma_8 \Omega_m^{0.6} \approx \text{const}$

$\Omega_m = 0.3$ fixed, flat Universe:

$\sigma_8 = 0.85 \pm 0.06$

[Hoekstra et al. 2006]

CTIO lensing survey

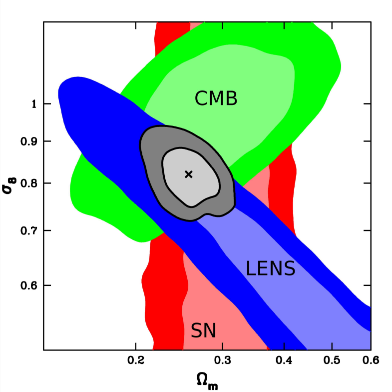

flat Universe

[Jarvis, Jain & Bernstein 2006]

$\Omega_m - w$

CFHTLS Wide

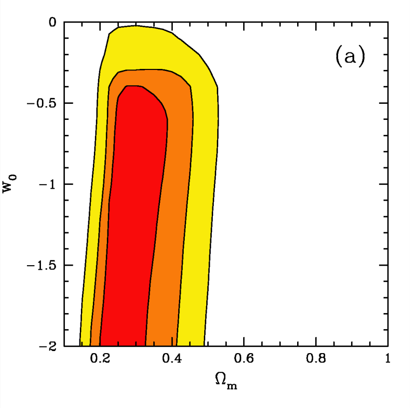

[Hoekstra et al. 2006]

CTIO lensing survey

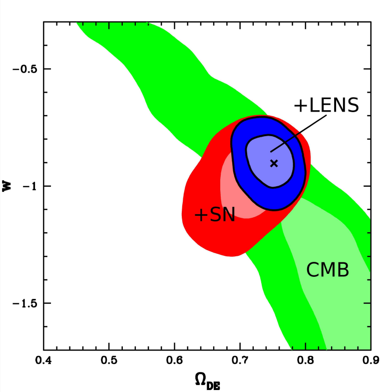

[Jarvis, Jain & Bernstein 2006]

Lift degeneracies

Lifting near-degeneracies by

- combining weak lensing with other experiments (CMB, SNIa, ...)
- shear tomography
- combining second- and third-order statistics

Scatter in σ_8

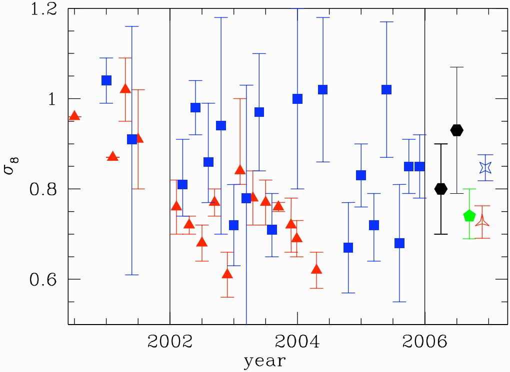

galaxy clusters
cosmic shear
GaBoDS cosmic shear
WMAP3

[Hetterscheidt et al. 2006]

Scatter in σ_8 from WL larger than error bars? Problem with systematics, e.g. calibration of shear amplitude? $\rightarrow$ STEP project

Redshift distribution $p(z)$

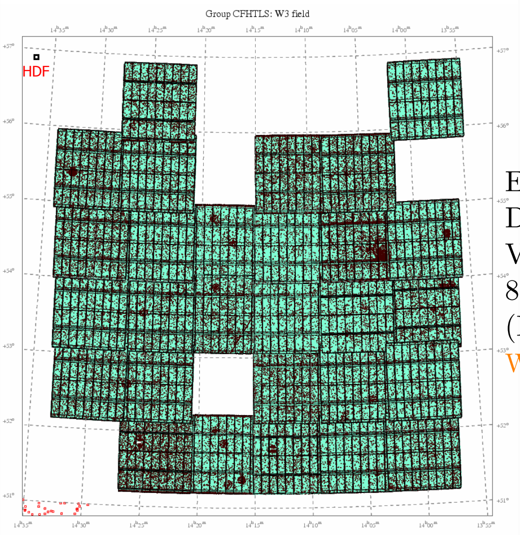

Even with 4 deg^2 (CFHTLS Deep, calibrated with VVSD): cosmic variance 2 – 8 $\times$ larger than statistical (Poisson) error [van Waerbeke et al. 2007]

. . . until recently from HDF.

Cosmic variance: wrong $p(z)$ biases measured σ_8.

Determination of parameters

Likelihood function (posterior)

Gaussian likelihood

$$\mathcal{L}(\boldsymbol{d};\boldsymbol{p}) = \frac{1}{\sqrt{(2\pi)^n \det C}} \exp[-\chi^2(\boldsymbol{d};\boldsymbol{p})/2]$$

Log-likelihood

$$\Delta\chi^2(\boldsymbol{d};\boldsymbol{p}) = \left(\boldsymbol{d}(\boldsymbol{p}) - \boldsymbol{d}^{\rm obs}\right)^{\rm t} C^{-1} \left(d(\boldsymbol{p}) - \boldsymbol{d}^{\rm obs}\right)$$

$\boldsymbol{d}$: data vector, e.g. $d_i = \xi(\vartheta_i), \langle M_{\rm ap}^2\rangle(\theta_i)$
C : covariance matrix, $C = \langle d d^{\rm t}\rangle - \langle d\rangle\langle d^{\rm t}\rangle$
$\boldsymbol{p}$: vector of cosmological parameters, e.g. $\Omega_{\rm m}, \sigma_8, h, w \ldots$

The E- and the B-mode

Convergence κ and shear γ are both second derivatives of the lensing potential ψ. Relation exists

$$\nabla\kappa = \begin{pmatrix} \partial_1\gamma_1 + \partial_2\gamma_2 \\ \partial_2\gamma_1 - \partial_1\gamma_2 \end{pmatrix} = \boldsymbol{u}$$

The vector $\boldsymbol{u}$ is the gradient of "potential" κ, therefore

$$\nabla \times \boldsymbol{u} = 0$$

$\rightarrow$ Gravitational lensing produces only gradient component (E-mode).

But: Measured $\boldsymbol{u}$ from data will not be curl-free due to measurement errors, systematics, noise, second-order effects, intrinsic shape correlations.

Use this curl-component (B-mode) to assess data quality!

Separating the E- and B-mode

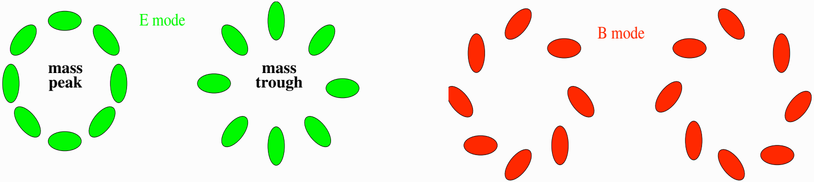

- Local measure for E- and B-mode: $\langle M_{\rm ap}^2 \rangle$
- Remember: $M_{\rm ap}(\theta) = \int \mathrm{d}^2\vartheta \, Q_\theta(\vartheta)\gamma_{\rm t}(\boldsymbol{\vartheta})$.
- Define: $M_\times(\theta) = \int \mathrm{d}^2\vartheta \, Q_\theta(\vartheta)\gamma_\times(\boldsymbol{\vartheta})$.
- Dispersion $\langle M_\times^2 \rangle$ is only sensitive to B-mode, i.e., vanishes if there is no B-mode.

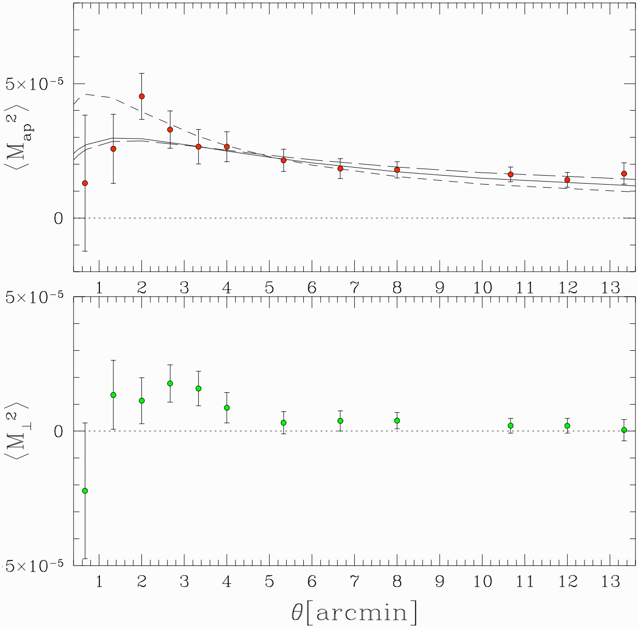

VIRMOS survey, CFHT, 6.5 deg^2, $I_{\rm AB} = 24.5$ [van Waerbeke et al. 2001]

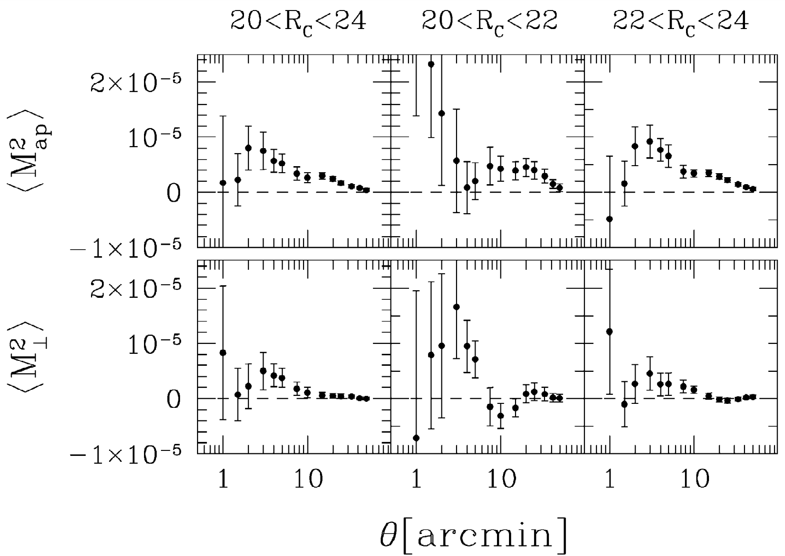

RCS survey, CFHT+CTIO, 53 deg^2, $R_C = 24$
[Hoekstra et al. 2002]

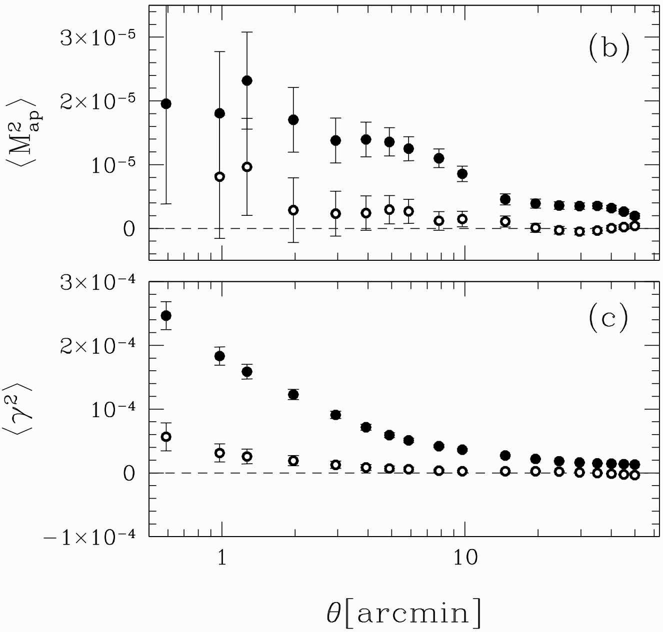

VIRMOS survey, CFHT, 8.5 deg^2, $I_{\rm AB} = 24.5$ [van Waerbeke, Mellier & Hoekstra 2005]

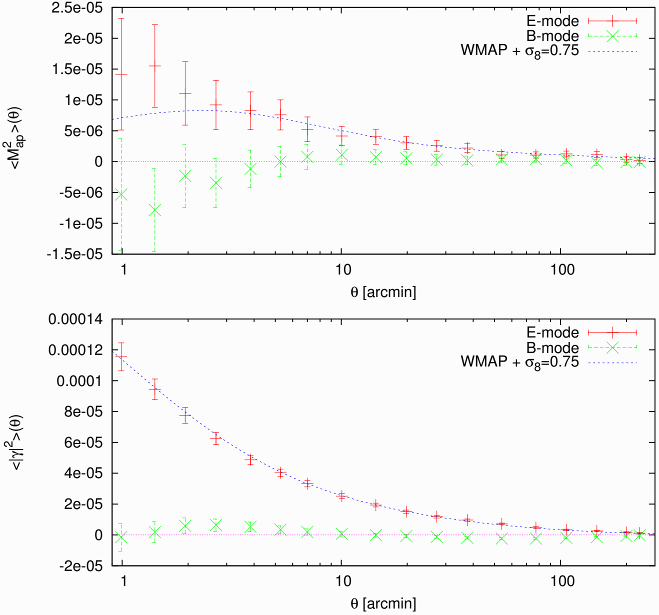

CFHTLS W3,
18 deg^2,
$I_{\mathrm{AB}} = 24.5$
[Fu et al. 2007 (in prep.)]

Shear tomography (2 1/2 D lensing)

If redshifts of source galaxies are known ...

- Divide galaxies into $i = 1 \ldots n$ redshift bins
- Measure power spectrum (shear statistics) from different bins P_κ^{ii} and cross-spectra P_κ^{ij}

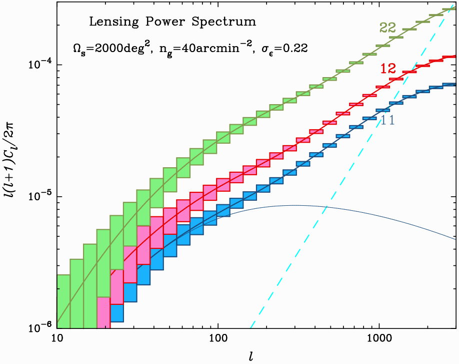

[Jain, Connnolly & Takada 2007]

- Different projections of LSS, different redshift ranges → evolution of structure growth, dark energy evolution, lift parameter degeneracies

Redshift binning

Requirements

- Redshifts do not have to be very accurate for individual galaxy but: systematics have to be well controlled!
  → photometric redshifts using a few (3-10) broad-band filters are sufficient (more later)
- Redshift bins can be broad and overlap, but distribution has to be known fairly accurately! (E.g. bias of mean z_{bias} and dispersion σ_z. Higher moments?)
- Small number of redshift bins sufficient, $n = 2$ already huge improvement

Improvement on parameter constraints

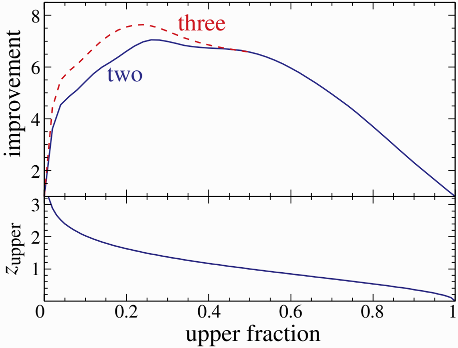

Improvement from shear tomography on error of Ω_Λ

p_α	$\sigma_\alpha f_{\rm sky}^{1/2}$	Error Improvement					
	1	$2(\frac{1}{2})$	$2(\frac{1}{4})$	$2(\frac{1}{8})$	$3(\frac{1}{3})$	$3(\frac{1}{4})$	$3(\frac{1}{8})$
Ω_Λ	0.040	6.5	6.9	5.7	7.2	7.7	6.9
Ω_K	0.023	2.9	3.1	2.9	3.3	3.5	3.2
m_ν	0.044	1.7	2.0	2.1	2.1	2.2	2.2
$\ln A$	0.064	1.7	2.0	2.0	2.1	2.2	2.1

[Hu 1999]

Results on shear tomography so far ... not many

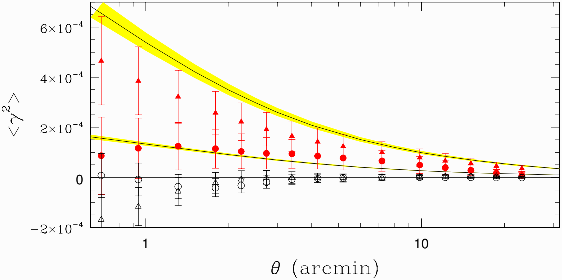

CFHTLS Wide
Shear "tomography"
using one band
(magnitude binning)
[Semboloni et al. 2006]

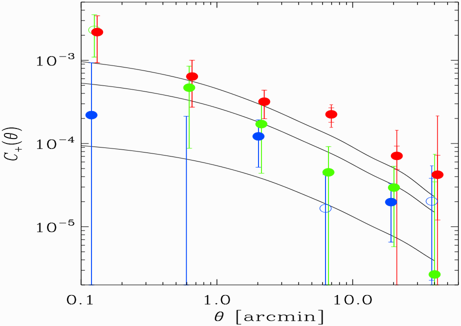

COSMOS: 1.6 □, observed by HST, Spitzer, GALEX, XMM, Chandra, Subaru, VLA, VLT, UKIRT, NOAO, CTHT, ... from radio to X-ray

Many bands from UV to IR
[Massey et al. 2007]

Lensing tomography with clusters

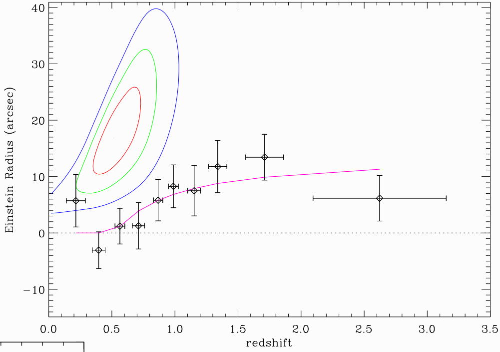

CFHTLS Deep
Weak lensing signal from a cluster using ugriz
[Gavazzi & Soucail 2007]

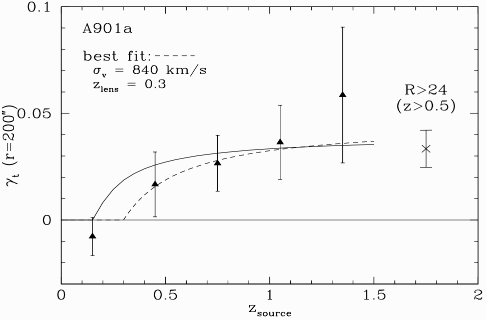

COSMO17
17 bands (5 broad, 12 medium)
[Taylor et al. 2004]

Growth of structure

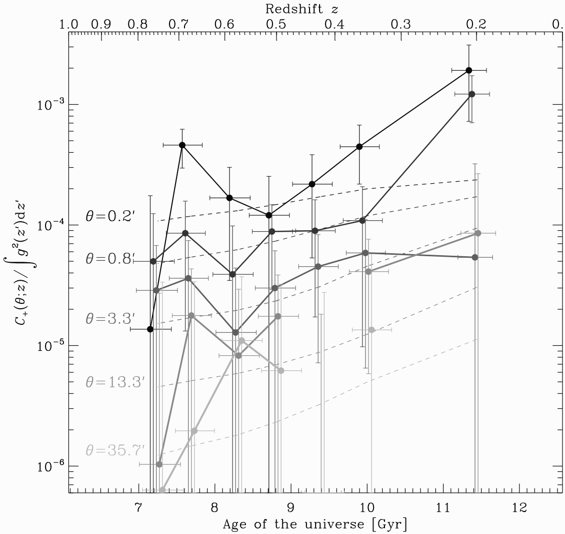

COSMOS, [Massey et al. 2007]

Third-order cosmic shear statistics

- Second-order shear statistics probes power spectrum $P_\kappa(\ell)$
- Third-order statistics probes bispectrum $B_\kappa(\ell_1, \ell_2, \ell_3) = B_\kappa(\ell_1, \ell_2, \cos\beta)$

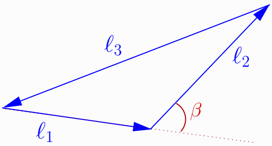

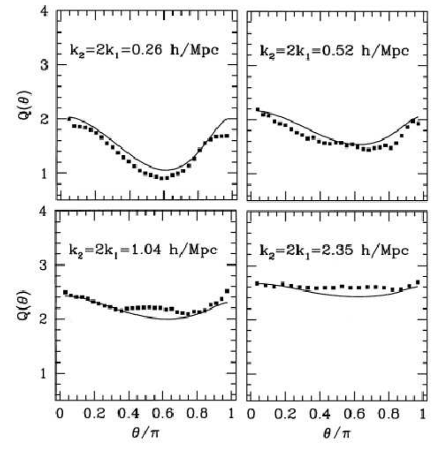

Reduced bispectrum, depends on triangle configuration

Bispectrum: Probing the cosmic web

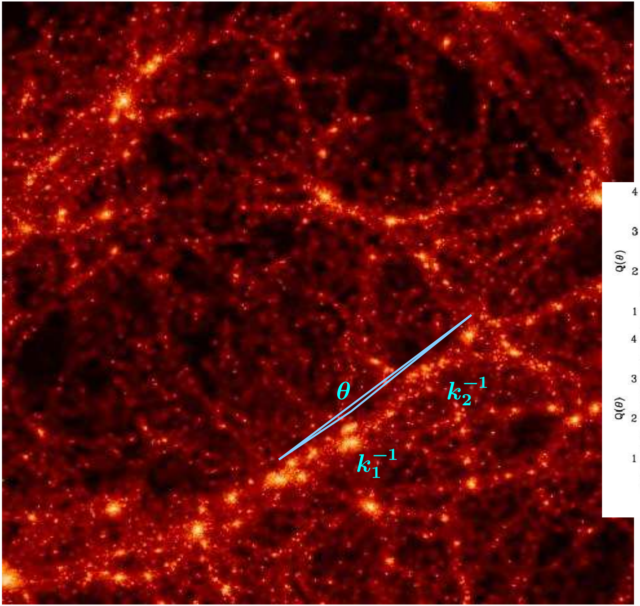

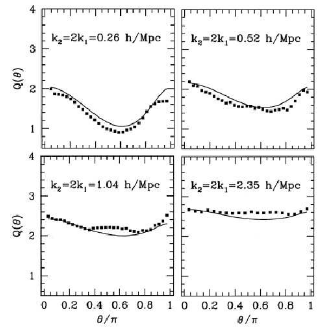

Bispectrum: Probing the cosmic web

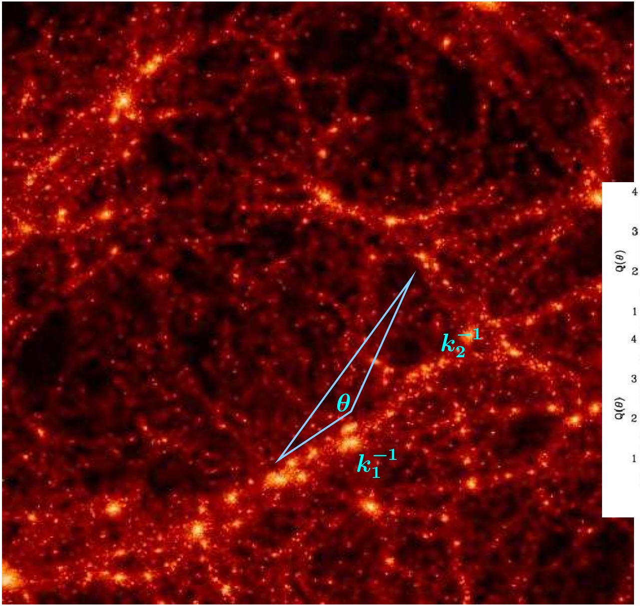

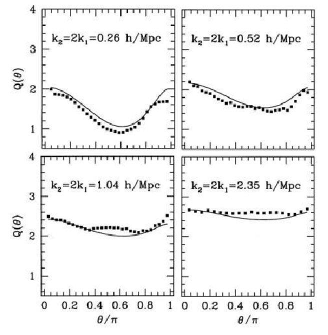

Bispectrum: Probing the cosmic web

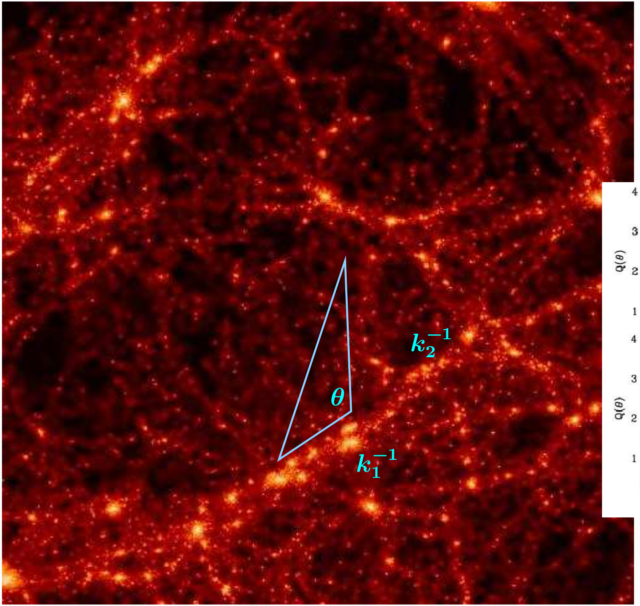

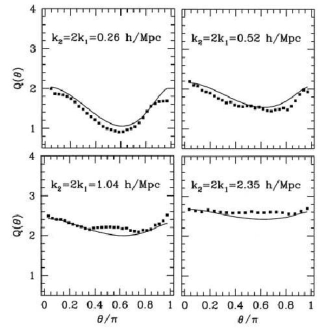

Bispectrum: Probing the cosmic web

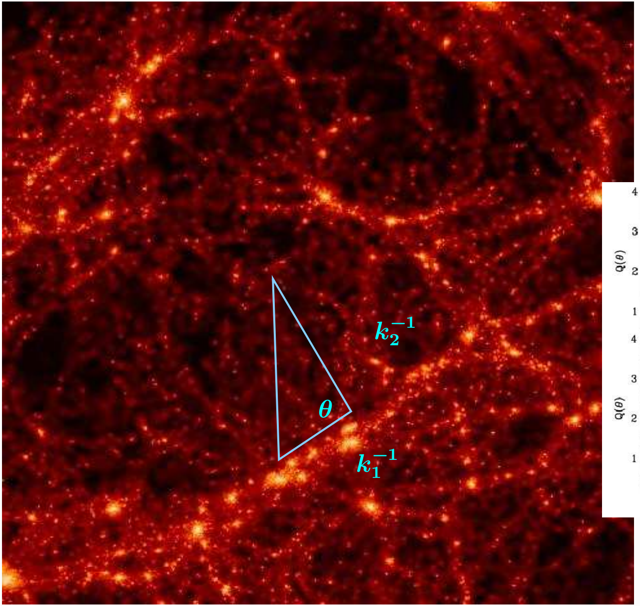

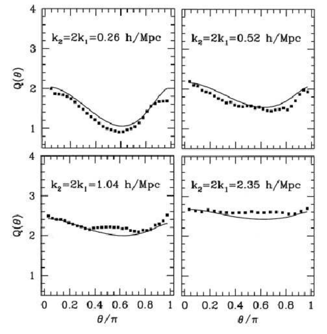

Bispectrum: Probing the cosmic web

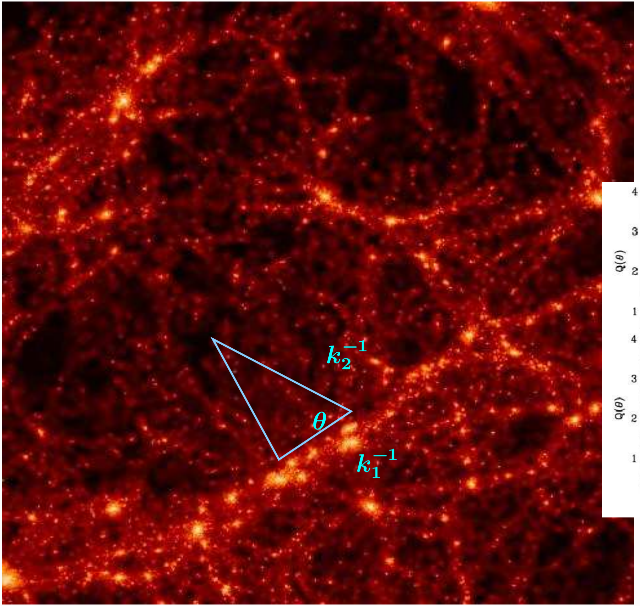

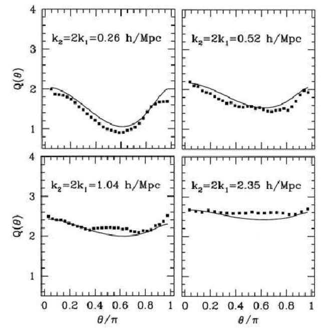

Bispectrum: Probing the cosmic web

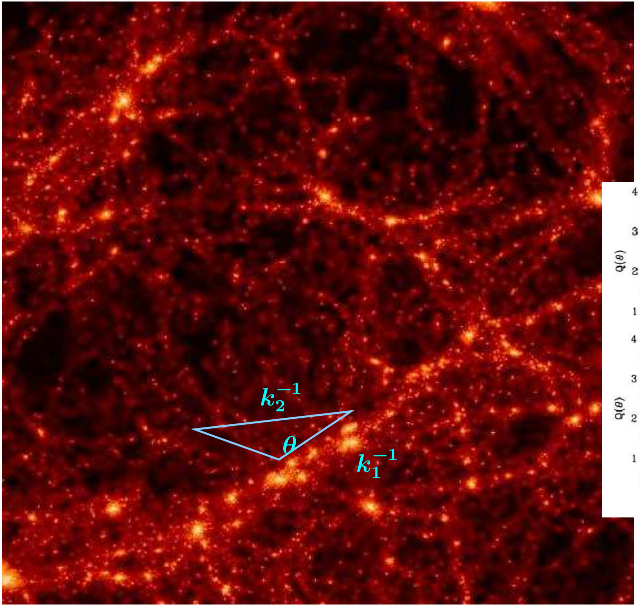

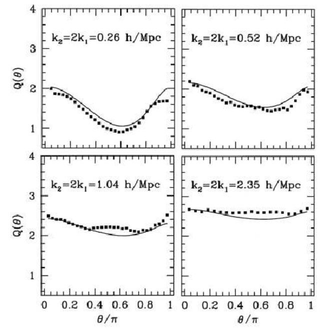

Bispectrum: Probing the cosmic web

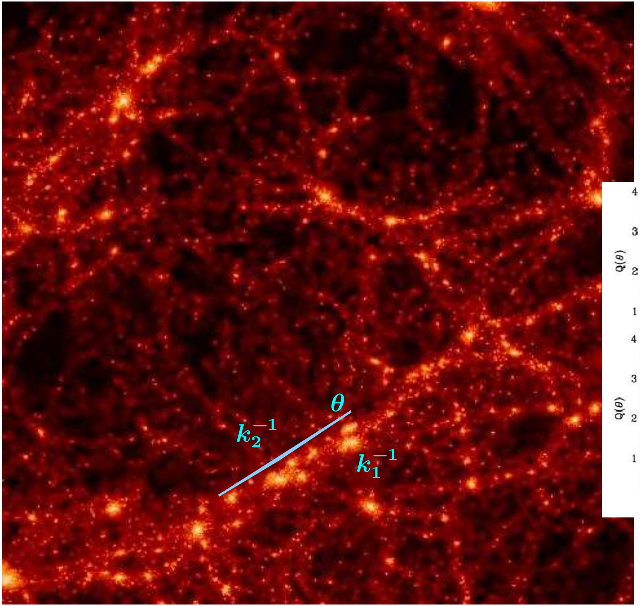

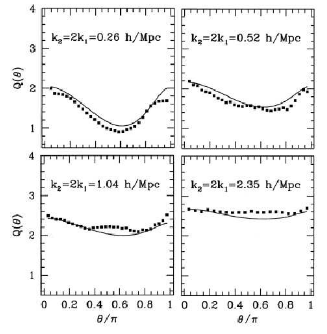

Bispectrum: Probing the cosmic web

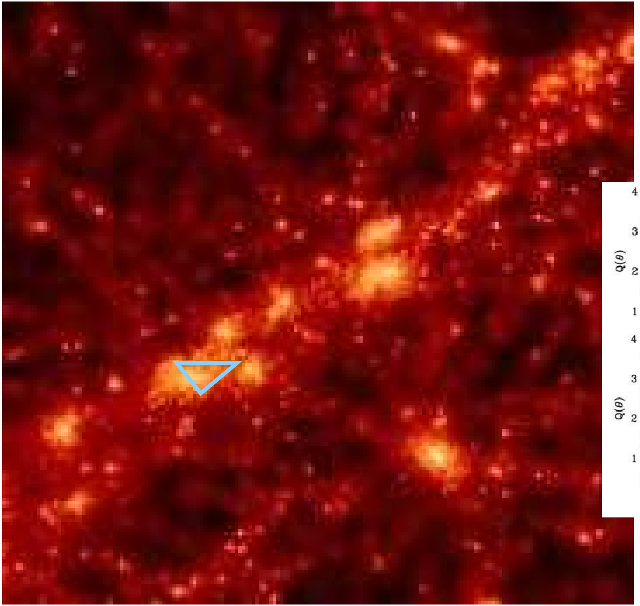

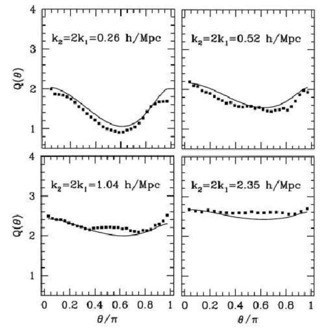

Three-point correlation function (3PCF)

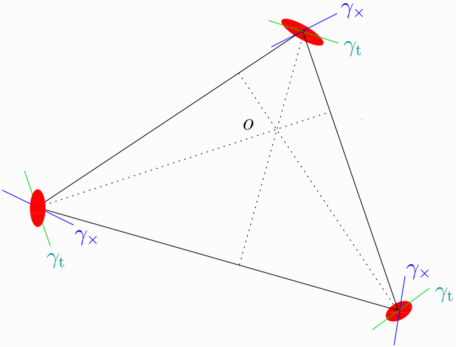

8 components:

$\langle\gamma_t\gamma_t\gamma_t\rangle$ $\langle\gamma_t\gamma_t\gamma_\times\rangle$
$\langle\gamma_t\gamma_\times\gamma_\times\rangle$ $\langle\gamma_t\gamma_\times\gamma_t\rangle$
$\langle\gamma_\times\gamma_t\gamma_\times\rangle$ $\langle\gamma_\times\gamma_t\gamma_t\rangle$
$\langle\gamma_\times\gamma_\times\gamma_t\rangle$ $\langle\gamma_\times\gamma_\times\gamma_\times\rangle$

't' and '×' with respect to (some) center of triangle

- "Natural components" $\Gamma^{(0)}, \Gamma^{(1)}, \Gamma^{(2)}, \Gamma^{(3)} \in \mathbb{C}$ = linear combinations of the $\langle\gamma_\mu\gamma_\nu\gamma_\lambda\rangle$ [Schneider & Lombardi 2003]
- 3PCF has 8 (non-vanishing) components, depends on 3 quantities and is not a scalar [SL03, Takada & Jain 2003, Zaldarriaga & Scoccimarro 2003]

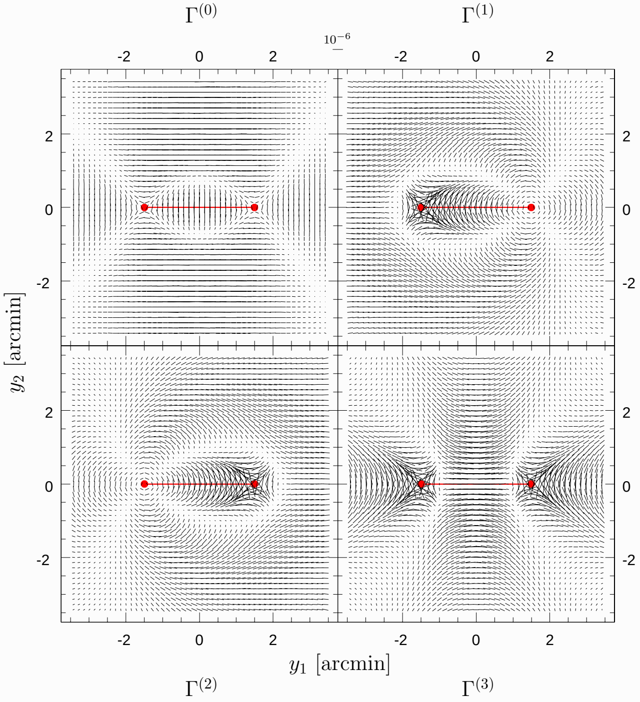

$\Gamma^{(0)}$
$\Gamma^{(1)}$
10^{-6}
-2
0
2
y_2 [arcmin]
y_1 [arcmin]
$\Gamma^{(2)}$
$\Gamma^{(3)}$

Flavors of 3$^{\text{rd}}$-order statistics

Projected 3PCF, integrated over elliptical region [Bernardeau, van Waerbeke & Mellier 2002, 2003]

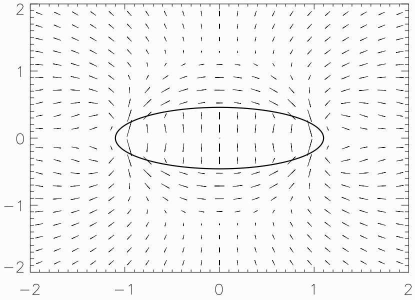

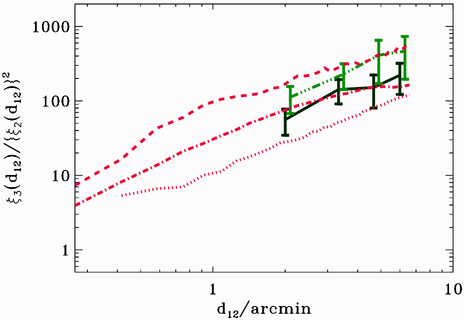

[VIRMOS-DESCART] Measurement consistent with ΛCDM

Aperture-mass skewness

- $\langle M_{\rm ap}^3\rangle(\theta)$ probes convergence bispectrum $B_\kappa(\ell_1 \propto 1/\theta, \ell_2 \propto 1/\theta, \ell_3 \propto 1/\theta)$
- Generalized skewness $\langle M_{\rm ap}^3\rangle(\theta_1, \theta_2, \theta_3) = \langle M_{\rm ap}(\theta_1) M_{\rm ap}(\theta_2) M_{\rm ap}(\theta_3)\rangle$ probes bispectrum $B_\kappa(\ell_1 \propto 1/\theta_1,\ \ell_2 \propto 1/\theta_2,\ \ell_3 \propto 1/\theta_3)$, cross-correlation or mode coupling of the large-scale structure on different scales [Schneider, MK & Lombardi 2005, MK & Schneider 2005]

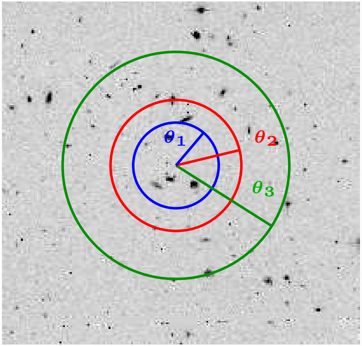

- E- and B-mode components: $\langle M_{\rm ap}^3 \rangle$, $\langle M_{\rm ap} M_\times^2 \rangle$, $\langle M_{\rm ap}^2 M_\times \rangle$, $\langle M_\times^3 \rangle$
- Quantities with odd power in $M_\times$ should vanish if shear field is parity-invariant

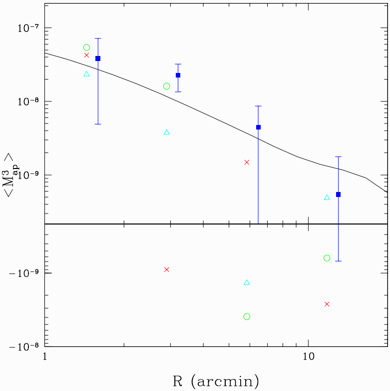

[CTIO, Jarvis et al. 2004]

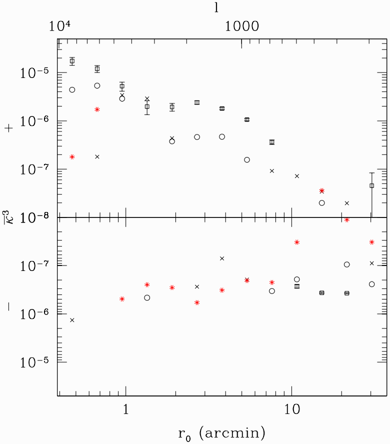

[VIRMOS, Pen et al. 2003]

Properties of $\langle M_{\rm ap}^3 \rangle$

- $\langle M_{\rm ap}^3 \rangle$ is scalar (3PCF: spin-2 and spin-6)
- separates E- & B-mode
- one can obtain $\langle M_{\rm ap}^3 \rangle$ from 3PCF
- $\langle M_{\rm ap}^3 \rangle$ contains same amount of information than 3PCF: 3PCF not sensitive to power on large scales
- Skewness of LSS (asymmetry between peaks and troughs) can be probed with aperture-mass skewness

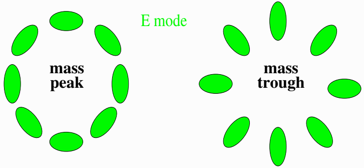

Third-order statistics and cosmology

- On small scales: Need non-linear model. E.g.: HEPT (Hyper-Extended Perturbation Theory) [Scoccimarro & Couchman 2001], halomodel
- Non-linear models not (yet) good enough for %-precision cosmology
- On large scales: Signal too small to measure?
- Source-lens clustering worrying (if not fatal) contamination to lensing skewness

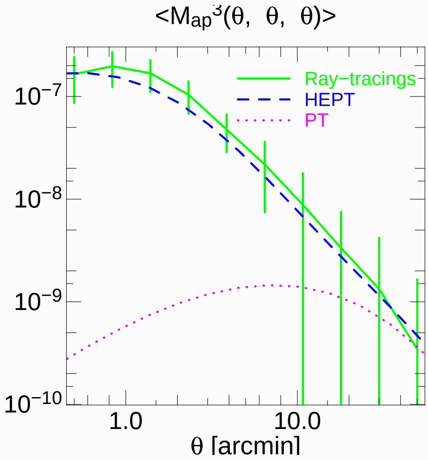

Predictions for CFHTLS Wide (very optimistic ...)

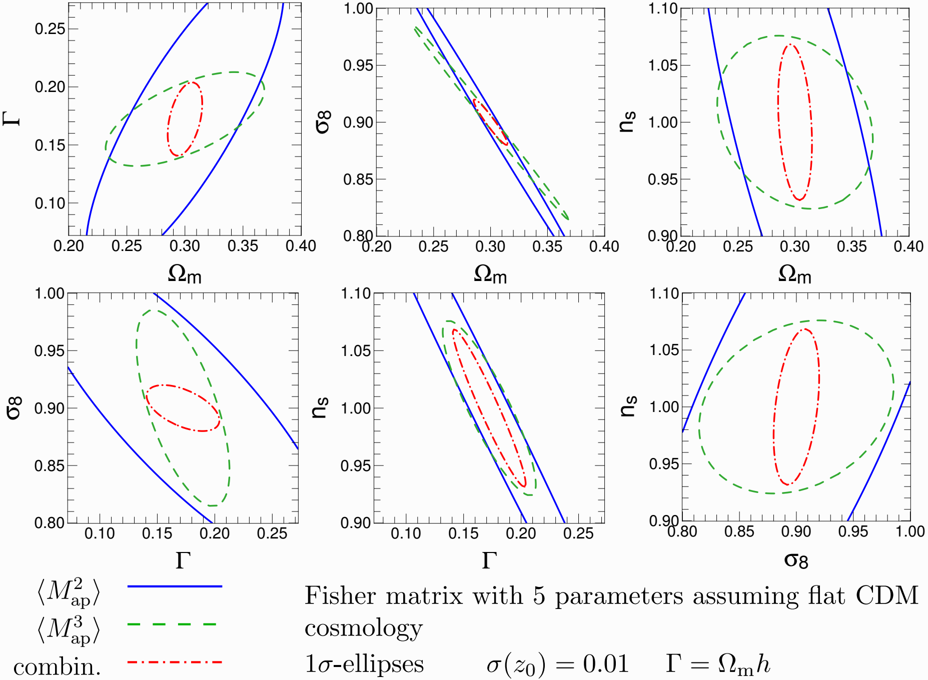

Fisher matrix with 5 parameters assuming flat CDM cosmology

1σ-ellipses $\quad \sigma(z_0) = 0.01 \quad \Gamma = \Omega_{\rm m} h$

More predictions (even more optimistic ...)

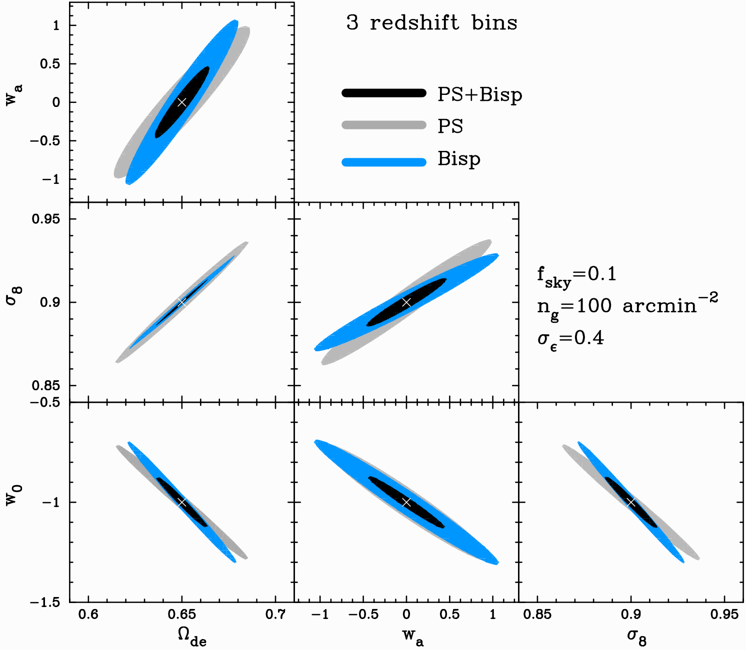

[Takada & Jain 2004]

Primordial Non-Gaussianity from lensing?

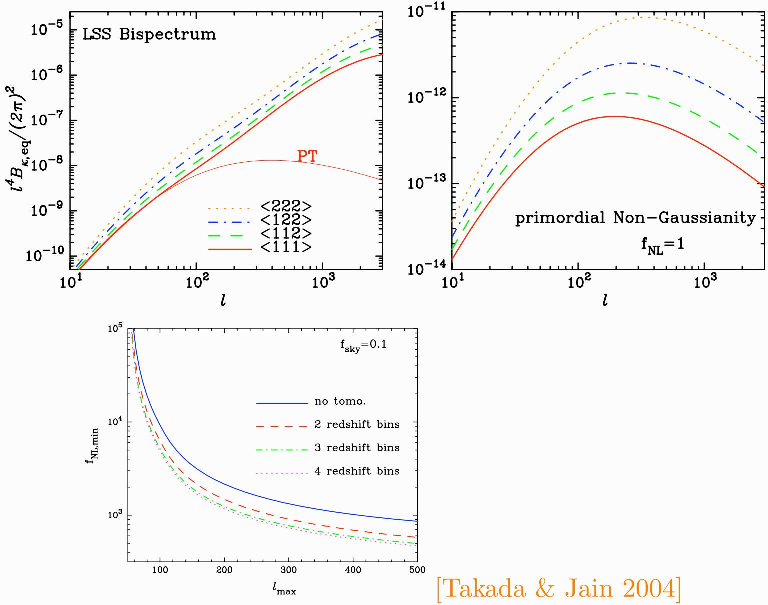

[Takada & Jain 2004]

Principle of 3D lensing

[Heavens 2003, Heavens et al. 2006]

- Spherical transformation of the 3D shear field, sampled at galaxy positions $(\boldsymbol{\vartheta}_i, w_i)$ (flat Universe)

$$\hat{\gamma}(\boldsymbol{\ell}, k) = \sqrt{\frac{2}{\pi}} \sum_i \gamma(\boldsymbol{\vartheta}_i, w_i)\, \mathrm{j}_\ell(k w_i) \exp(-\mathrm{i}\boldsymbol{\vartheta}\boldsymbol{\ell})$$

  Comoving distance w_i from (photometric) redshift z_{ph} and fiducial cosmological model

- Log-Likelihood

$$\Delta\chi^2 = \sum_{\boldsymbol{\ell},k,k'} \left[\ln \det C_\ell(k,k') + \hat{\gamma}^{\mathrm{t}}(\boldsymbol{\ell},k)\, C_\ell^{-1}(k,k')\, \hat{\gamma}(\boldsymbol{\ell},k)\right]$$

  assuming different ℓ-modes are uncorrelated.

- Covariance matrix is sum of signal and noise term, $C = S + N$
- Note: The data vector has zero expectation, $\langle\hat{\gamma}\rangle = 0$! All information is contained in the (signal) covariance matrix C_ℓ which depends on the 3D power spectrum P_δ. [C.f. CMB anisotropies]
- Applied to COMBO-17 survey (proof of concept)

COMBO-17

- 5 broad-band filters (UBVRI) + 17 medium-band filters for excellent photo-zs
- 4 selected fields each $30' \times 30'$ using WFI @ MPG/ESO 2.2m, $R = 24$ (for lensing)

3D lensing: first results

Solid: 3D lensing (2 fields)
Dashed: 2D lensing (3 fields)

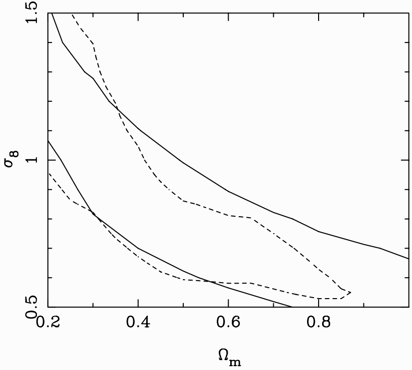

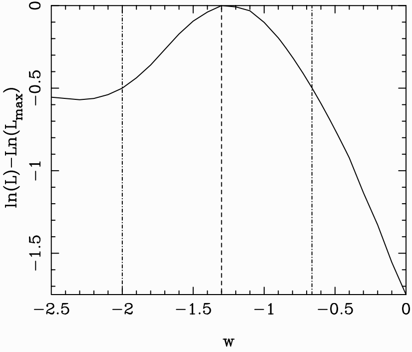

COMBO-17 [Kitching et al. 2007]

Peak statistics

A shear-selected sample of halos ($M \gtrsim 10^{13.5} M_\odot$) can be used to constrain cosmological parameters by comparing to theoretical mass function $n(M, z)$.

- Galaxy clusters: matter density, normalization σ_8, dark energy evolution and BAO can be measured
- Shear might be better proxy for mass than richness, σ_v, L_X, T_X, SZ signal, ... Independent of morphology, dynamical state, galaxy formation.
- CDM N-body simulations for calibration [Hennawi & Spergel 2005]

Detecting peaks

- Measure filtered γ_t in annuli

$$M(\boldsymbol{\zeta}, \theta) = \int \mathrm{d}^2\vartheta\, Q_\theta(\vartheta)\gamma_\mathrm{t}(\boldsymbol{\vartheta} - \boldsymbol{\vartheta}),$$

- Look for peaks in this "M"-map higher than some S/N-threshold ν.
- Choices for Q:
  - compensated filter (M_ap), lower limit on mass
  - matched filter ($Q \propto \gamma_\mathrm{t}(\mathrm{N}FW)$), high efficiency

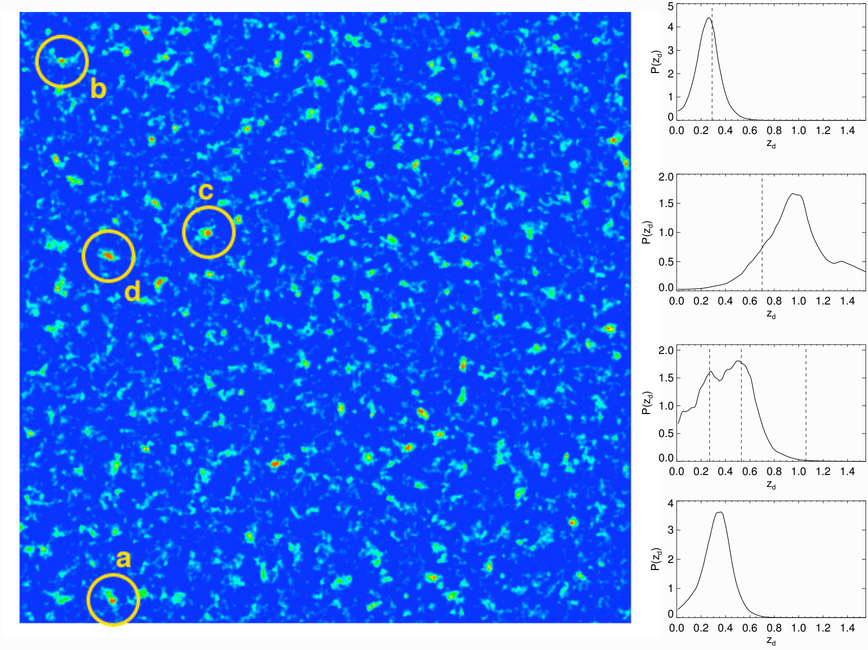

b
c
d
a
P(z_d)
z_d
0.0 0.2 0.4 0.6 0.8 1.0 1.2 1.4

- Main difficulty: Noise (intrinsic ellipticty and LSS/chance projections) increases $n_{\rm peak}(\nu)$!
- Efficiency $\varepsilon = n_{\rm halos}/n_{\rm peaks} \le 1$ (from simulations) because of many false positives
- The higher ν, the higher ε, but the lower the completeness.

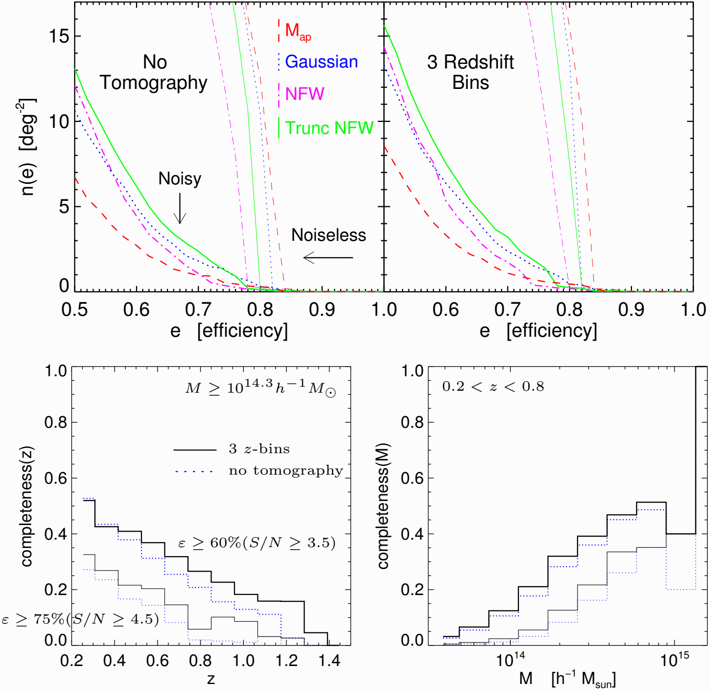

No Tomography
3 Redshift Bins
M_{ap}
Gaussian
NFW
Trunc NFW
Noisy
Noiseless
n(e) [deg^{-2}]
e [efficiency]
$M \geq 10^{14.3} h^{-1} M_\odot$
3 z-bins
no tomography
$\varepsilon \geq 60\% (S/N \geq 3.5)$
$\varepsilon \geq 75\% (S/N \geq 4.5)$
completeness(z)
z
$0.2 < z < 0.8$
completeness(M)
M [h^{-1} M$_{sun}$]

Cosmology with peak statistics

Problem:

Cannot just compare n_{peak} with theoretical mass function $n(M, z)$ because of false positives.

- Optical/X-ray follow-up to confirm galaxy cluster: introduces bias again, back to square one!
- Compare with n_{peak} from simulations. To fit cosmological parameters, need a grid of N-body simulations, expensive! But: Correlations between peaks not needed, simple and fast simulations maybe sufficient

Observations:

Shear-selected samples from DLS [Wittman et al. 2006], GaBoDS [Schirmer et al. 2007, Maturi et al. 2007], BLOX [Dietrich et al. 2007]

Cosmic shear & peak statistics

Question: Can combining cosmic shear with peak statistics improve parameters constraints? Isn't it not just sampling of the high-end part of the power spectrum?

Answer: No!

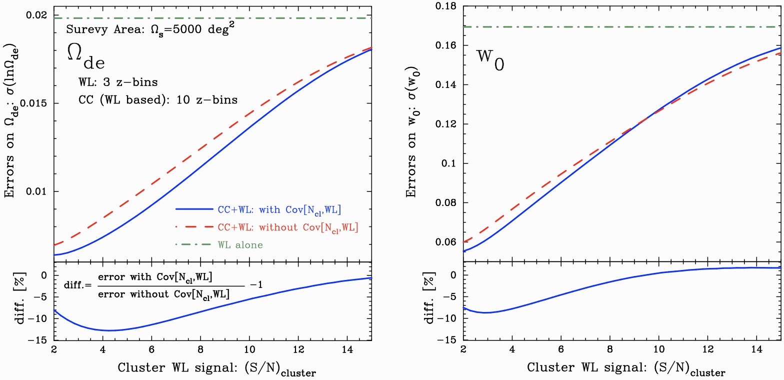

[Takada & Bridle 2007]

Shear-ratio geometry test

[Jain & Taylor 2003, Taylor et al. 2007]

The principle:

"The variation of the weak lensing signal with redshift around massive foreground objects depends solely on the angular diameter distances".

- Cross-correlation between tangential shear and halo (galaxy cluster)

$$w_{\rm t,h}(\theta) = \frac{1}{2\pi} \int_0^{w_{\rm lim}} \frac{{\rm d}w}{f_K(w)} \, n_{\rm f}(w) G(w) \int_0^\infty {\rm d}\ell \, \ell \, P_{\delta {\rm h}} \left(\frac{\ell}{f_K(w)}, w \right) {\rm J}_2(\theta\ell)$$

$$\left[\text{c.f.} \quad \xi_\pm(\theta) = \frac{1}{2\pi} \int {\rm d}w \, G^2(w) \int {\rm d}\ell \, \ell \, P_\delta \left(\frac{\ell}{f_K(w)}, w \right) {\rm J}_{0,4}(\theta\ell) \right]$$

Shear-ratio geometry test

- Lens efficiency

$$G(w) = \frac{3}{2}\left(\frac{H_0}{c}\right)^2 \frac{\Omega_\mathrm{m}}{a(w)} \int_w^{w_\mathrm{lim}} \mathrm{d}w'\, p(w') \frac{f_K(w'-w)}{f_K(w')}$$

for a single source redshift z: $w' \to w(z)$

$$G(w(z_\mathrm{l})) \propto \frac{f_K[w(z)-w(z_\mathrm{l})]}{a[w(z_\mathrm{l})] f_K[w(z)]}$$

- Plus single lens redshift z_l:

$$w_\mathrm{t,h}(\theta, z) \propto \frac{f_K[w(z)-w(z_\mathrm{l})]}{f_K[w(z)] a[w(z_\mathrm{l})] f_K[w(z)]} \int \mathrm{d}\ell\, \ell\, P_\delta[\ell, w(z_\mathrm{l})] \mathrm{J}_{0,4}(\theta\ell)$$

Shear-ratio geometry test

- Ratio of shear at two source redshifts

$$\frac{w_{\mathrm{t,h}}(z_1)}{w_{\mathrm{t,h}}(z_2)} = \frac{f_K[w(z_1) - w(z_\mathrm{l})]/f_K[w(z_1)]}{f_K[w(z_2) - w(z_\mathrm{l})]/f_K[w(z_2)]}$$

  is independent of halo details (mass, profile, ...) and angular distance θ. Clean measure of angular diameter distance as functions of redshift $\leftrightarrow$ geometry of the Universe.

- Simple signal-to-noise estimate: Assume only shot noise from intrinsic ellipticities:

$$\frac{S}{N} = \frac{\langle\gamma\rangle_{\mathrm{rms}}}{\sigma_\epsilon}\sqrt{N_\mathrm{g}} \approx 6\left(\frac{n_\mathrm{g}}{\mathrm{arcmin}^{-2}}\,\frac{A}{\deg^2}\right)^{1/2}$$

Shear-ratio geometry test

Advantages of this method

- High shear values (1% – 10%) around clusters
- First-order in γ, less sensitive to PSF effects, less stringent imaging requirements

Detailed error analysis must include

- shot-noise
- photo-z errors
- contribution from large-scale structure (cosmic shear):

First detection using three clusters (A901a, A901b, A902) in COMBO-17, $\gamma_{\mathrm{t}}(\theta, z)$ fitted to SIS profile [Kitching et al. 2007].

Observational aspects of weak lensing

Overview

- Shape measurement
- Photometric redshifts
- Intrinsic alignment
- Non-linear structure formation
- Non-Gaussian errors

(Leiden list)

Measuring ellipticity

Reminder:
Weak gravitational lensing causes small image distortions.
(Linearized) lens mapping: circle → ellipse.

Need to measure "ellipticity" for irregular shaped objects such as faint, high-redshift galaxies...

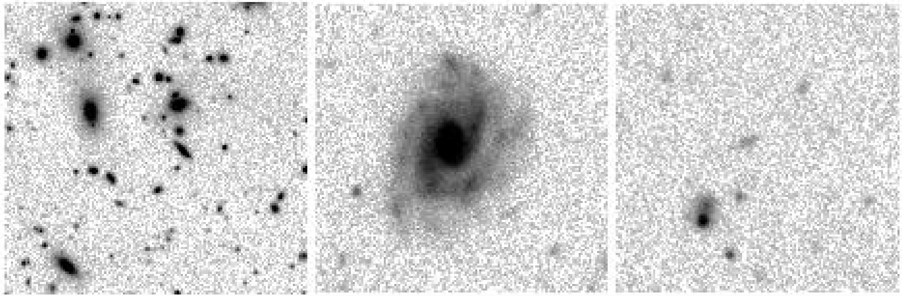

[Y. Mellier]

Defining ellipticity

- Second-order tensor of brightness distribution

$$Q_{ij} = \frac{\int \mathrm{d}^2\theta\, q[I(\boldsymbol{\theta})]\,(\theta_i - \bar{\theta}_i)(\theta_j - \bar{\theta}_j)}{\int \mathrm{d}^2\,\theta\, q[I(\boldsymbol{\theta})]}, \quad i, j = 1, 2$$

$I(\boldsymbol{\theta})$: brightness distribution of galaxy

q : weight function

$$\bar{\boldsymbol{\theta}} = \frac{\int \mathrm{d}^2\theta\, q_I[I(\boldsymbol{\theta})]\,\boldsymbol{\theta}}{\int \mathrm{d}^2\theta\, q_I[I(\boldsymbol{\theta})]} : \quad \text{barycenter}$$

- Ellipticity

$$\varepsilon = \frac{Q_{11} - Q_{22} + 2\mathrm{i}Q_{12}}{Q_{11} + Q_{22} + 2(Q_{11}Q_{22} - Q_{12}^2)^{1/2}}$$

- Circular object $Q_{11} = Q_{22}, Q_{12} = Q_{21} = 0$
- Elliptical isophotes, axis ratio r: $|\varepsilon| = (1 - r)/(1 + r)$

From source to image

- Analogously define $Q^{\rm s}_{ij}$ for source brightness
- With lens equation:

$$Q^{\rm s} = \mathcal{A} Q \mathcal{A}$$

[Reminder:

$$\mathcal{A} = \begin{pmatrix} 1-\kappa-\gamma_1 & -\gamma_2 \\ -\gamma_2 & 1-\kappa+\gamma_1 \end{pmatrix} = (1-\kappa) \begin{pmatrix} 1-g_1 & -g_2 \\ -g_2 & 1+g_1 \end{pmatrix}$$

Jacobi-matrix of mapping between lens and source position. Reduced shear $g_i = \gamma_i/(1-\kappa)$]

- Relation between source $\varepsilon^{\rm s}$ and image ellipticity ε

$$\varepsilon^{\rm s} = \begin{cases} \dfrac{\varepsilon - g}{1 - g^* \varepsilon} & \text{for} \quad |g| \le 1 \\[2ex] \dfrac{1 - g\varepsilon^*}{\varepsilon^* - g^*} & \text{for} \quad |g| > 1 \end{cases},$$

- weak-lensing regime: $\kappa, |\gamma| \ll 1 \rightarrow \varepsilon \approx \varepsilon^{\rm s} + \gamma$

Measuring second-order shear

Estimators

- 2PCF: correlate all galaxy pairs

$$\hat{\xi}_\pm(\vartheta) = \frac{1}{N_\mathrm{pair}} \sum_{\substack{ij \\ \text{pairs} \in \vartheta-\text{bin}}}^{N_\mathrm{pair}} \left(\varepsilon_{i\mathrm{t}} \varepsilon_{j\mathrm{t}} \pm \varepsilon_{i\times} \varepsilon_{j\times} \right)$$

- Aperture-mass dispersion: place apertures over data field

$$\hat{M}(\theta) = \frac{1}{N_\mathrm{ap}} \sum_{n=1}^{N_\mathrm{ap}} \frac{1}{N_n(N_n - 1)} \sum_{\substack{i \neq j \\ \text{gal} \in \text{ap.}}}^{N_n} Q_i Q_j \varepsilon_{i\mathrm{t}} \varepsilon^*_{j\mathrm{t}}$$

(tophat-variance similar)

Interrelations

Placing apertures very inefficient due to gaps, masking. Correlating pairs for 2PCF makes optimal use of data.

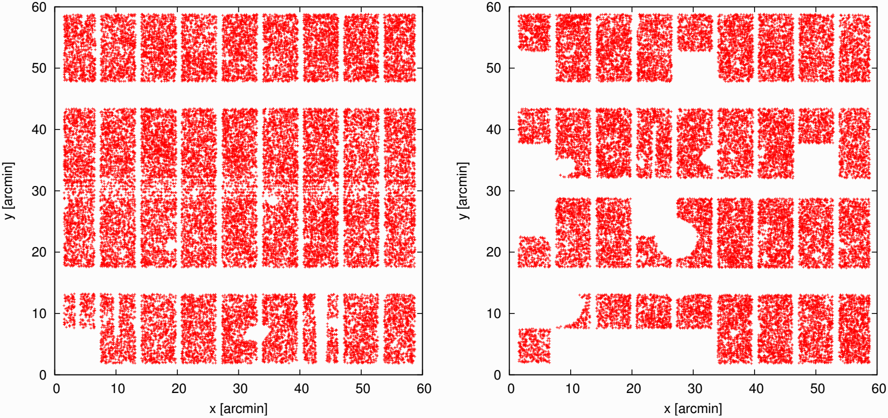

Invert relation between 2PCF and power spectrum $\longrightarrow$ express aperture measures in terms of 2PCF

Interrelations

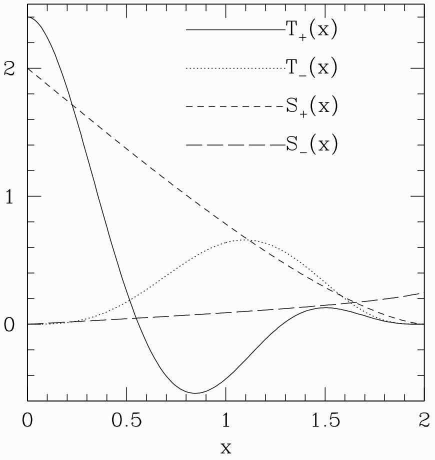

$T_\pm, S_\pm$ depend on $\hat{U}$, analytical expressions exist

$$\langle M_{\rm ap}^2 \rangle(\theta) = \int_0^{2\theta} \frac{\mathrm{d}\vartheta\,\vartheta}{\theta^2}\, T_+\left(\frac{\vartheta}{\theta}\right) \xi_+(\vartheta) = \int_0^{2\theta} \frac{\mathrm{d}\vartheta\,\vartheta}{\theta^2}\, T_-\left(\frac{\vartheta}{\theta}\right) \xi_-(\vartheta)$$

$$\langle |\gamma|^2 \rangle(\theta) = \int_0^{2\theta} \frac{\mathrm{d}\vartheta\,\vartheta}{\theta^2}\, S_+\left(\frac{\vartheta}{\theta}\right) \xi_+(\vartheta) = \int_0^{\infty} \frac{\mathrm{d}\vartheta\,\vartheta}{\theta^2}\, S_-\left(\frac{\vartheta}{\theta}\right) \xi_-(\vartheta)$$

Interrelations in the presence of a B-mode

$$\langle M_{\mathrm{ap},\times}^2\rangle(\theta) = \frac{1}{2}\left[\int_0^{2\theta} \frac{\mathrm{d}\vartheta\,\vartheta}{\theta^2}\,T_+\left(\frac{\vartheta}{\theta}\right)\xi_+(\vartheta)\ \pm\ \int_0^{2\theta} \frac{\mathrm{d}\vartheta\,\vartheta}{\theta^2}\,T_-\left(\frac{\vartheta}{\theta}\right)\xi_-(\vartheta)\right]$$

$$\langle|\gamma|^2\rangle_{\mathrm{E,B}}(\theta) = \frac{1}{2}\left[\int_0^{2\theta} \frac{\mathrm{d}\vartheta\,\vartheta}{\theta^2}\,S_+\left(\frac{\vartheta}{\theta}\right)\xi_+(\vartheta)\ \pm\ \int_0^{\infty} \frac{\mathrm{d}\vartheta\,\vartheta}{\theta^2}\,S_-\left(\frac{\vartheta}{\theta}\right)\xi_-(\vartheta)\right]$$

$$\xi_{\mathrm{E,B}}(\theta) = \frac{1}{2}\left[\xi_+(\theta)\ \pm\ \xi_-(\theta) \pm \int_\theta^{\infty} \frac{\mathrm{d}\vartheta}{\vartheta}\xi_-(\vartheta)\left(4 - 12\frac{\theta^2}{\vartheta^2}\right)\right]$$

Top-hat-variance and corr. function not local!

E- and B-mode mixing

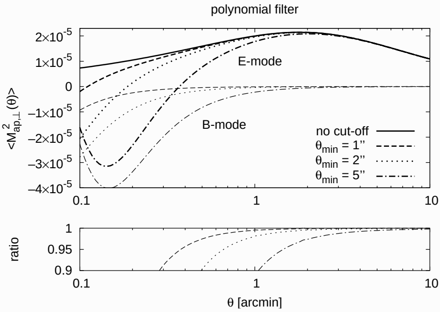

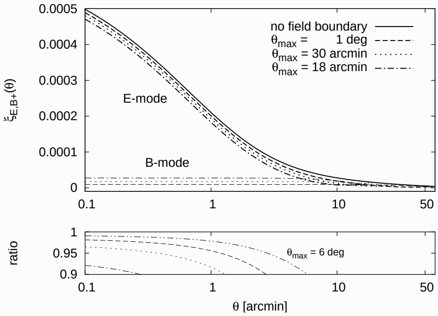

Aperture-mass statistics: B-mode on small scales due to minimum angular scales (blending of galaxy images) [MK, Schneider & Eifler 2006]

Correlation function and top-hat-variance: ≈ constant B-mode on all scales due to maximum scale (field size)

E-/B-mode separation on finite angular range: Ring statistics [Schneider & MK 2006]

PSF effects

The problem:

- Need to measure galaxy shapes to percent-level accuracy.
- Galaxies are faint ($I > 21$), small ($\gtrsim$ arcsec = few pixel) and are
  1. smeared by seeing
  2. distorted by instrumental imperfections: defocusing, abberation, coma etc., tracking errors, chip not planar, image coaddition

  Effect:
  1. Makes galaxies rounder
  2. Mimics a shear signal $\gg \gamma$!

  Solution:
  1. Seeing $\lesssim 1''$
  2. Correct for PSF anisotropies

Example of star images

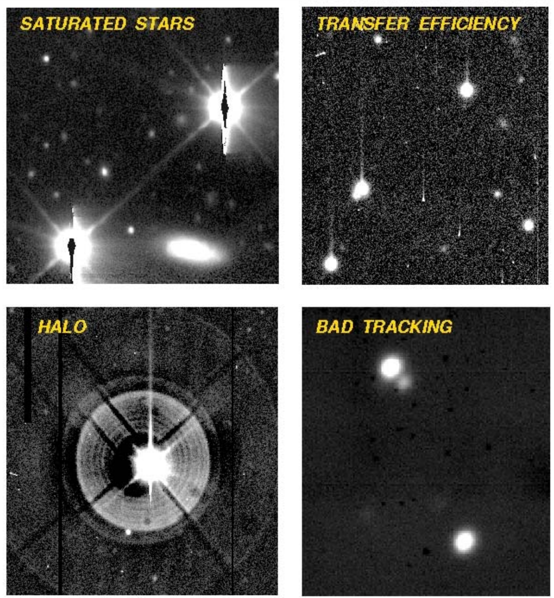

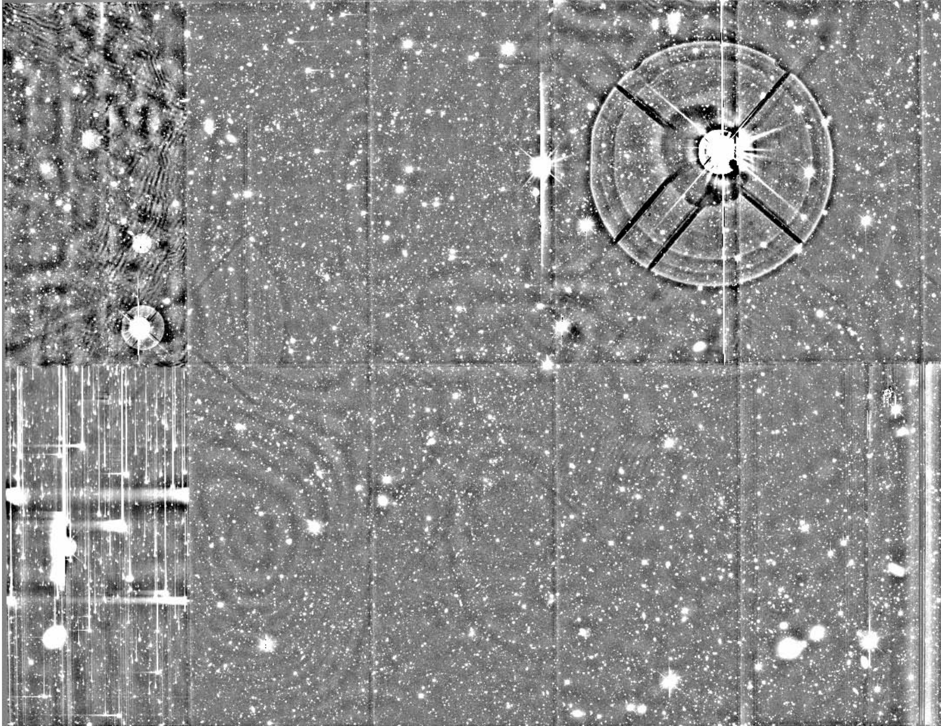

KSB

[Kaiser, Squires & Broadhurst 1995]: Perturbative ansatz for PSF effects

$$\varepsilon^{\rm obs} = \varepsilon^{\rm s} + P^{\rm sm}\varepsilon^* + P^{\rm sh}\gamma$$

[c.f. $\varepsilon^{\rm obs} = \varepsilon^{\rm s} + \gamma$ from before]

$P^{\rm sm}$	smear polarisability, (linear) response of to ellipticity to PSF anisotropy
e^*	PSF anisotropy
$P^{\rm sh}$	shear polarisability, isotropic seeing correction
γ	shear

$P^{\rm sm}, P^{\rm sh}$ are functions of galaxy brightness distribution.
e^*: fit function (polynomial/rational) to star PSFs, extrapolate to galaxy positions

PSF effects depend on galaxy ...

- size
- magnitude
- morphology
- SED (color gradient within broad-band filter)

Object selection

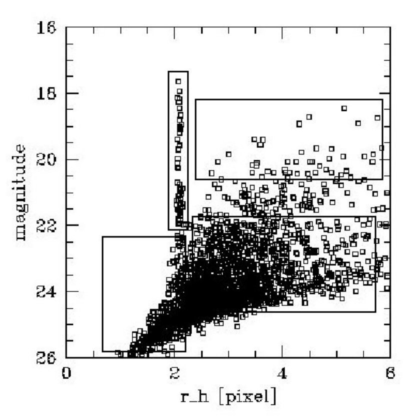

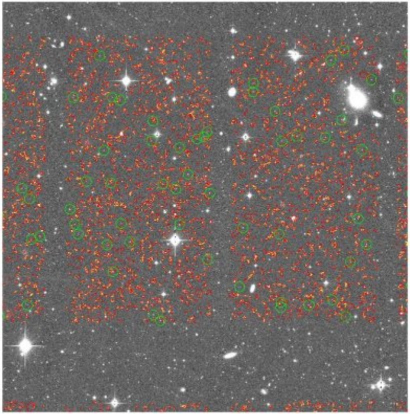

CFHTLS Wide [I. Tereno]

From size-magnitude diagram select galaxies and stars.

PSF pattern

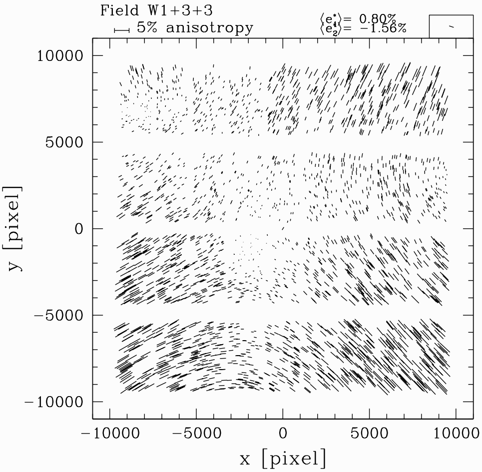

PSF correction works if

- PSF pattern is smooth (can be fitted by simple function)
- star density is high enough ($\sim$ 10-20 stars per chip)

[Hoekstra et al. 2006]

PSF correction

55 CFHTLS Wide pointings

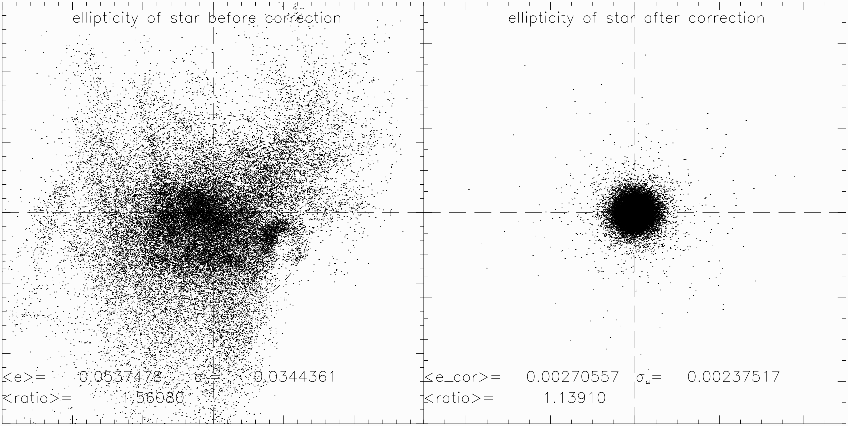

[Fu et al. 2007 (in prep.)]

KSB alternatives

Shapelets [Refregier 2003, Massey & Refregier 2003, Kuijken 2006]

- Decompose galaxies and stars into basis functions.

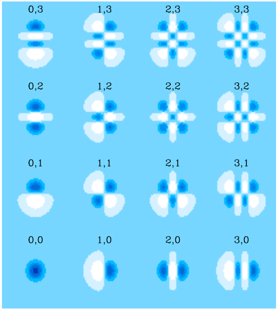

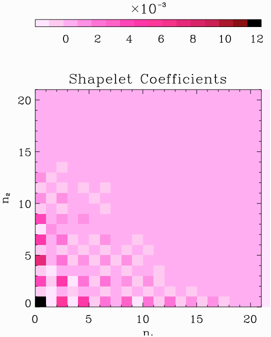

- PSF correction, convergence and shear acts on shapelet coefficients, deconvolution feasible
- Beyond second-order (quadrupole moment)

KSB alternatives

PCA decomposition [Bernstein & Jarvis 2002, Nakajima & Bernstein 2007]

Similar to shapelets method, but shears the basis functions until they match observed galaxy image

im2shape [Kuijken 1999, Bridle et al. 2002]

Fits sum of elliptical Gaussian to each galaxy (MCMC). In principle offers clean way to translate shape measurement errors into errors on cosmological parameters. But: Very slow!

Weak lensing from space

Advantages and disadvantages

- No seeing, resolution is diffraction-limited (HST: < 100 mas)
- Deeper (higher z, larger number density), better IR-coverage than from earth
- HST: PSF undersampled, 'ugly', time-variations
- small field of view, few stars
- CCD 'aging', many cosmic rays, CTE problems

Results

- Cluster WL: excellent results (high shear signal, calibration less crucial)
- Cosmic shear: COSMOS, GEMS, GOODS, ACS parallel survey

Space-based cosmic shear surveys

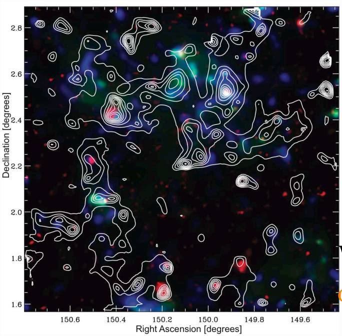

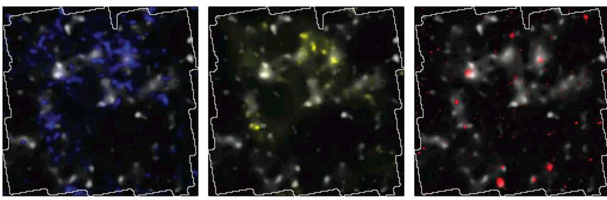

WL mass (contours), stellar mass, galaxy density, X-ray

[Massey et al. 2007]

STEP = Shear TEsting Programme

- World-wide collaboration of most of the weak lensing groups, started in 2004.
- Blind analysis of simulated images to test and calibrate different shape measurement methods, data reduction pipelines.

STEP 1	Simple Galaxy and PSF types	Heymans et al. 2006
STEP 2	Galaxy images with shapelets	
	Results from STEP 1 used	Massey et al. 2007
STEP 3	Space-based observations	in prep.
STEP 4	Back to the roots?	

…

STEP results

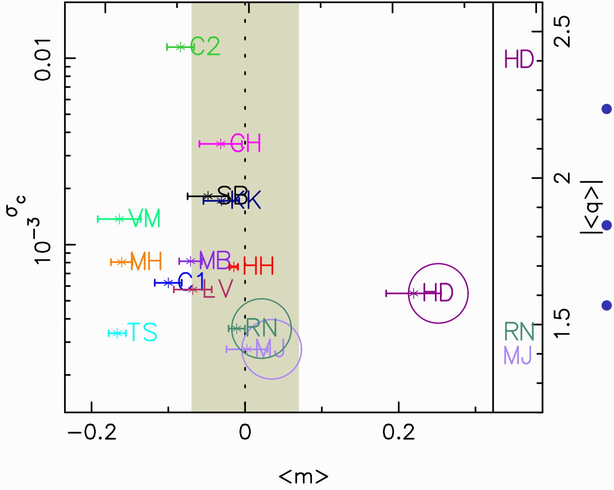

- Multiplicative m and additive errors σ_c, $\gamma^{\rm obs} - \gamma^{\rm true} = m\gamma^{\rm true} + c$
- Best methods measure better shear than 7%
- STEP 2: Sub-percent level not yet reached

Principle of photo-zs

- Redshifted galaxy spectra have different colors

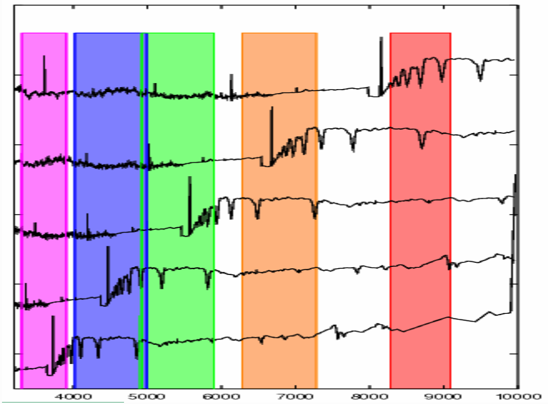

[from Y. Mellier]

- 4000 Å-break strongest feature → ellipticals (old stellar population) best, spirals ok, irregular/star-burst (emission lines) very unreliable

Photometric redshifts

- Redshift desert $z \approx 1.5 - 2.5$, neither 4000 Å-break nor Ly-break in visible range
- Confusion between low-z dwarf ellipticals and high-z galaxies
- Need UV band and IR for high redshifts! But: UV very insensitive, IR absorbed by atmosphere, have go to space
- Need database of galaxy spectra templates (observed or synthetic)
- Calibrate with spectroscopic galaxy sample. But always $N_{\rm spec} \ll N_{\rm WL}$

Photo-z calibration

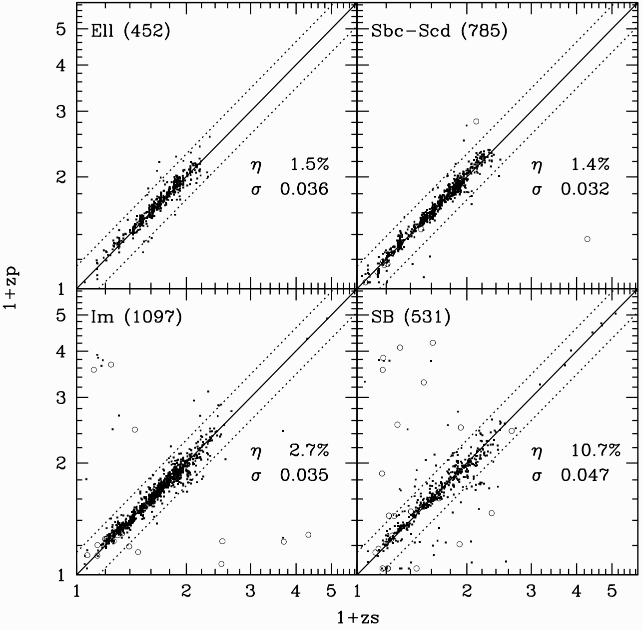

Minimize catastrophic failures

$$\frac{z_{\rm ph} - z}{1+z} \lesssim 0.5$$

$17.5 \leq i'_{AB} \leq 24$

[Ilbert et al. 2006]

Photometric errors and cosmology

Degradation of w_a-constraint as fct. of uncertainty
in photo-z parameters $\Delta z_{\text{bias}} = \Delta\sigma_z$

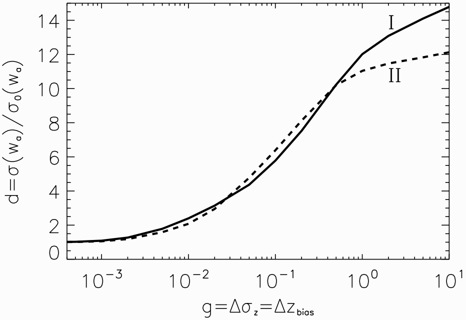

Cumulative number of galaxies in spectroscopic sample for degradation = 1.5

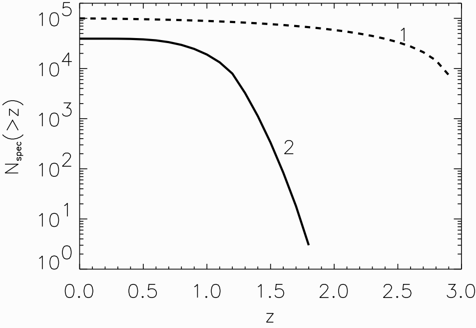

perfect redshifts:

$\sigma_0(w_a)$ =0.69 (I)

$\sigma_0(w_a)$ =0.96 (II)

[Ma, Hu & Huterer 2006]

Size of spectroscopic sample

Error on bias and dispersion in μ^{th} redshift bins

$$\Delta z^{\mu}_{\text{bias}} = \frac{\sigma^{\mu}_{z}(\text{ind. gal})}{\sqrt{N^{\mu}_{\text{spect}}}}$$

$$\Delta \sigma^{\mu}_{z} = \frac{\sigma^{\mu}_{z}(\text{ind. gal})}{\sqrt{N^{\mu}_{\text{spect}}/2}}$$

Assume $\sigma_z(\text{ind. gal}) = 0.1$, 5 photo-z bands. To reach $\Delta z^{\mu}_{\text{bias}} = 10^{-3}$, we need a total of $N_{\text{spec}} = 5 \cdot 10^4$ spectra!

Requirements for high-precision cosmology

- some 10^4 spectra to very faint magnitudes
- IR bands from space

Other possibilities

- Intermediate calibration step between ≈ 5 bands and spectra: large number of broad bands from UV to far-IR (10^3 spectra sufficient?)
- Angular correlation between photo-z bins to determine true z-distribution (e.g. correlation between low- and high-z bins $\leftarrow$ contamination by catastrophic outliers)

Intrinsic alignment

Intrinsic-intrinsic correlation (II)

- Reminder: basic equation of weak lensing $\varepsilon = \varepsilon^{\mathrm{s}} + \gamma$
- Second-order correlations

$$\langle \varepsilon_i \varepsilon_j^* \rangle = \langle \varepsilon_i^{\mathrm{s}} \varepsilon_j^{\mathrm{s}*} \rangle + \langle \varepsilon_i^{\mathrm{s}} \gamma_j^* \rangle + \langle \gamma_j \varepsilon_j^{\mathrm{s}*} \rangle + \langle \gamma_i \gamma_j^* \rangle$$

- $\langle \varepsilon_i^{\mathrm{s}} \varepsilon_j^{\mathrm{s}*} \rangle \neq 0$ for $z_i \approx z_j$, and if shapes of galaxies intrinsically correlated, e.g. through spin-coupling with dm halo, tidal torques
- II measured in COMBO-17 (Heymans et al. 2004), not measured in SDSS (Hirata et al. 2004). B-modes as diagnostics?
- Theoretical predictions do not agree with each other

Theoretical predictions of II-correlation

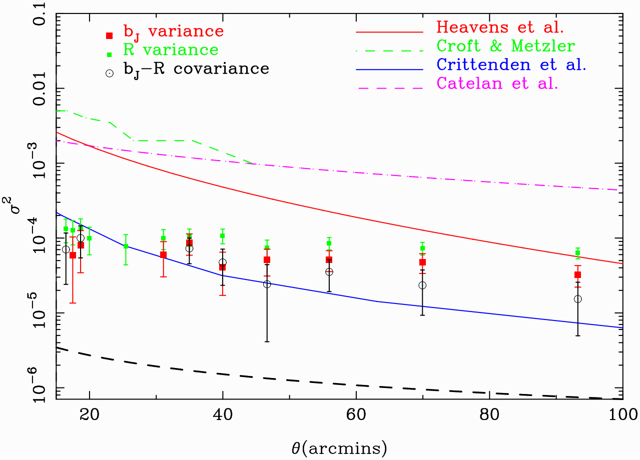

[Brown et al. 2002]

Conclusion

- II-contamination probably unimportant. Can be reduced by going deep, and down-weighting (physically) close pairs (photo-zs!)

Intrinsic-shear correlation (GI)

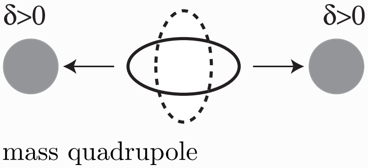

- $\langle \varepsilon_i^{\rm s} \gamma_j^* \rangle \neq 0$ for $z_i < z_j$, and if foreground galaxy aligned with its halo that causes lensing signal

- Anti-correlation between background shear and foreground orientation $\rightarrow$ underestimate σ_8 by up to 10%
- Unlike II, GI cannot be down-weighted!

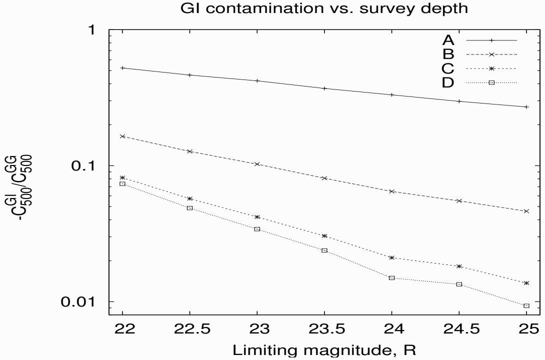

[Hirata et al. 2004, 2007] SDSS+2SLAQ

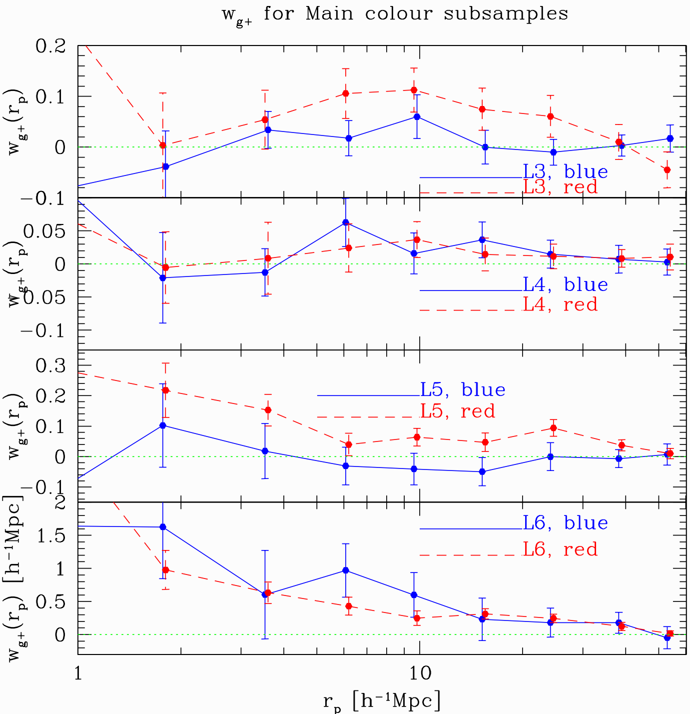

w_{g+} for Main colour subsamples
0.2
0.1
0
−0.1
0.05
0
−0.05
−0.1
0.3
0.2
0.1
0
−0.1
2
1.5
1
0.5
0
w_{g+}(r_p)
w_{g+}(r_p) [h^{-1}Mpc]
L3, blue
L3, red
L4, blue
L4, red
L5, blue
L5, red
L6, blue
L6, red
1
10
r_p [h^{-1}Mpc]

Non-linear structure formation

Problems

- Non-linear predictions of dark-matter P_δ not better than $\approx 5\%$ on small scales [Peacock&Dodds 1996, Smith, Peacock et al. 2003]
- With baryonic physics much worse!
- Dark energy dependence not really tested, extrapolations valid?
- Accuracy of non-linear bispectrum B_δ $15 - 30\%$ [Scoccimarro & Couchman 2001]
- Halo model, semi-analytic, works also for higher-order statistics, but many fine-tuning parameters

Necessary accuracy of P_δ not to be dominated by systematic errors in P_δ (@ $k \sim 1$ h/Mpc).

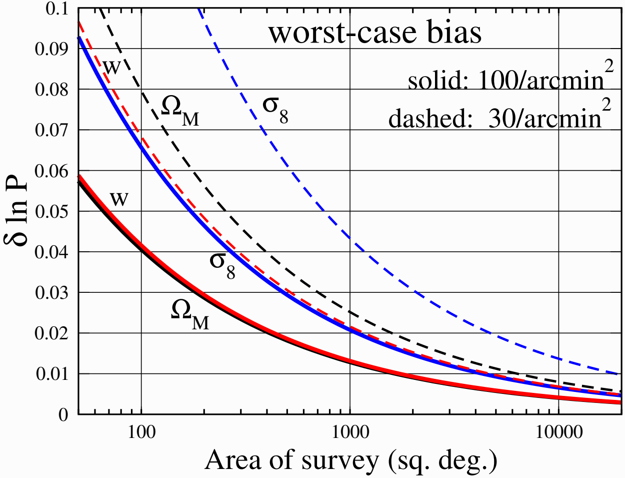

[Huterer & Takada 2005]

Non-Gaussian errors

- Second-order correlations

$$\langle \varepsilon_i \varepsilon_j^* \rangle = \langle \varepsilon_i^{\rm s} \varepsilon_j^{\rm s*} \rangle + \langle \gamma_i \gamma_j^* \rangle = \sigma_\varepsilon^2 \delta_{ij} + \xi_+(\vartheta_{ij})$$

- Error of second-order correlations is square of above. Schematically:

$$\begin{aligned} \mathrm{cov} &= c_1\, \sigma_\varepsilon^4 + c_2\, \sigma_\varepsilon^2\, \langle \gamma\gamma \rangle + c_3\, \langle \gamma\gamma\gamma\gamma \rangle \\ &\equiv D + M + V \end{aligned}$$

D : 'diagonal term', shot noise due to intrinsic ellipticity and finite numbers of galaxies

M : mixed term

V : sample "cosmic" variance, due to finite observed volume

Cosmic variance term V

If shear field were Gaussian: $V = 3\,\langle\gamma\gamma\rangle^2$, cov known analytically [Schneider, van Waerbeke, MK & Mellier]. But this is not the case! What is $\langle\gamma\gamma\gamma\gamma\rangle_{\rm c}$?

Possible ways to get $V_{\rm non-Gauss}$:

- Field-to-field variance from data, if large number of independent patches observed
- From ray-tracing simulations
- Fitting formulae [Semboloni et al. 2007]
- Cov. of P_κ, fourth-order statistics from halo-model, [e.g. Cooray & Hu 2001]

Covariance for CFHTLS Wide, 55 deg^2

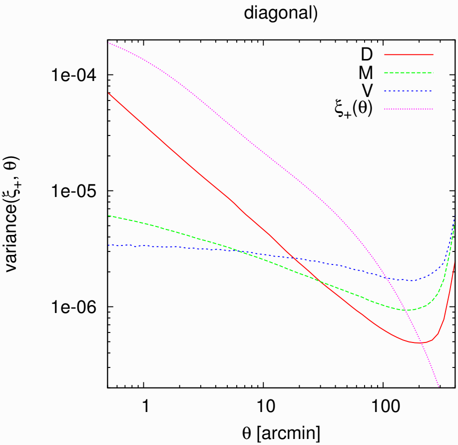

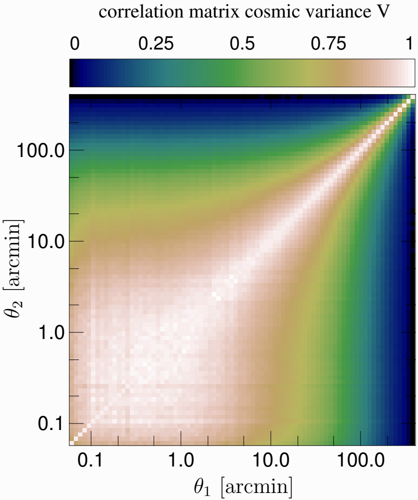

Non-Gaussian cosmic variance important on small scales

$\langle M_{\mathrm{ap}}^2 \rangle$, survey area = 3 square degree

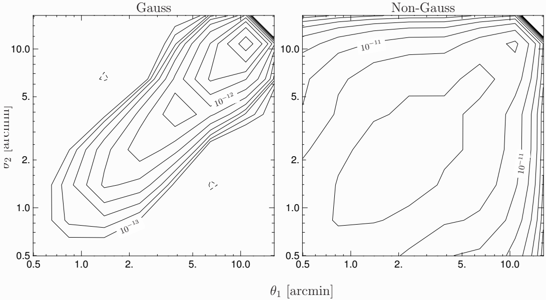

[MK & Schneider 2005]

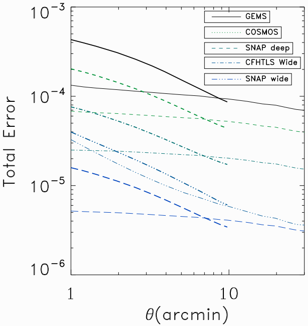

[Semboloni et al. 2007]

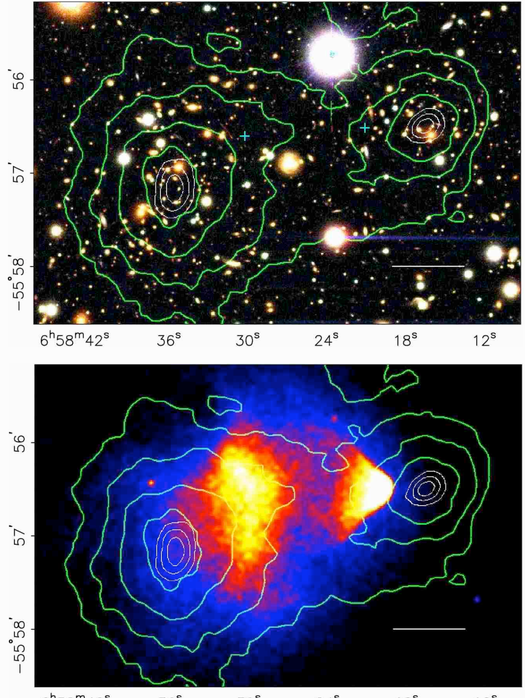
56′
57′
−55°58′
6h58m42s
36s
30s
24s
18s
12s
56′
57′
−55°58′

Results from the bullet cluster

- Combined strong+weak lensing, optical, X-ray analysis [Bradač et al., Clowe et al. 2006]
- Self-interaction of dark matter: $\sigma/m < 1.25\mathrm{cm\ g}^{-1}$ [Randall et al. 2007]
- [Angus, Shan, Zhao & Famaey 2007]: MOND + 2 eV hot neutrinos as collisionless dark matter, falsifiable by KATRIN β-decay experiment by 2009. Not a new idea [Sanders 2003, McGaugh 2004]

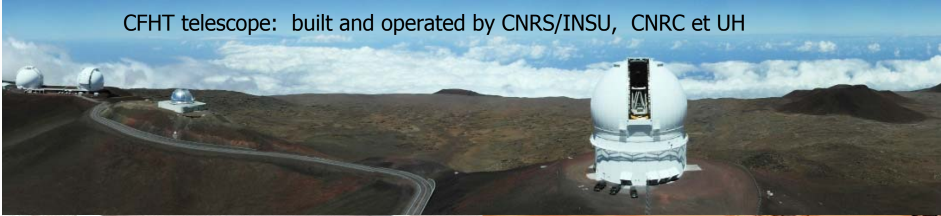
CFHT telescope: built and operated by CNRS/INSU, CNRC et UH

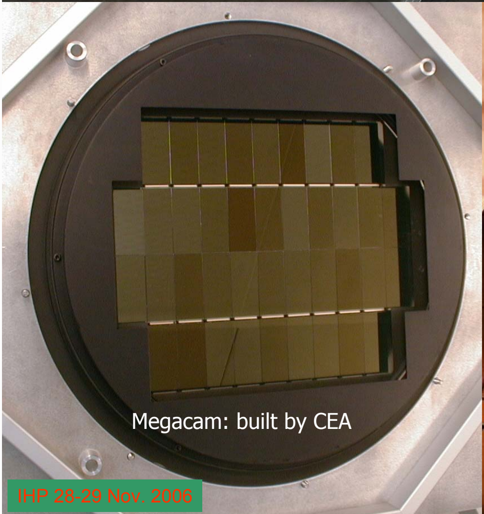
Megacam: built by CEA

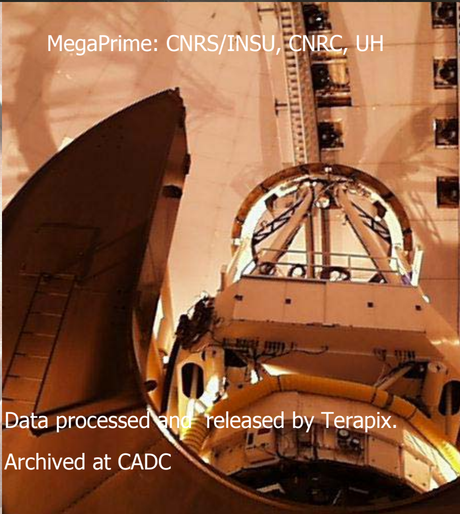
MegaPrime: CNRS/INSU, CNRC, UH
Data processed and released by Terapix.
Archived at CADC

Canada-France-Hawaii Telescope Legacy Survey: Canada-France collaboration

- 3 champs W de 50 deg^2 (CFHTLS-Wide), 4 champs de 1 deg^2 (CFHTLS-Deep)
- 500 nuits entre Juin 2003 and Juin 2008 (temps de télescope CNRS/INSU+CNRC)

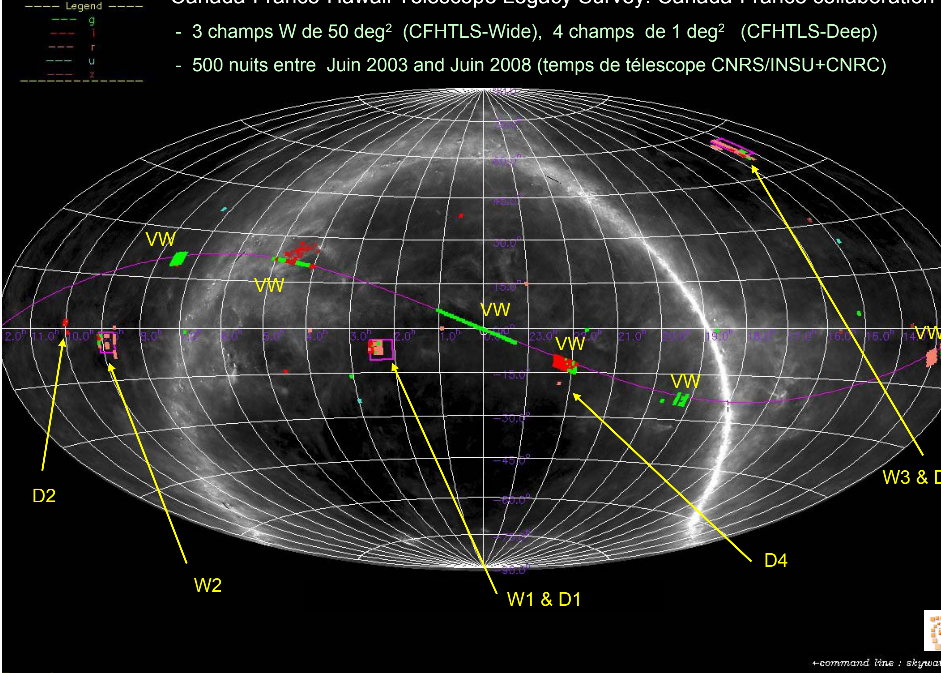

Terapix/Skywatcher : all data 03A-05A : 20000 Megacam images

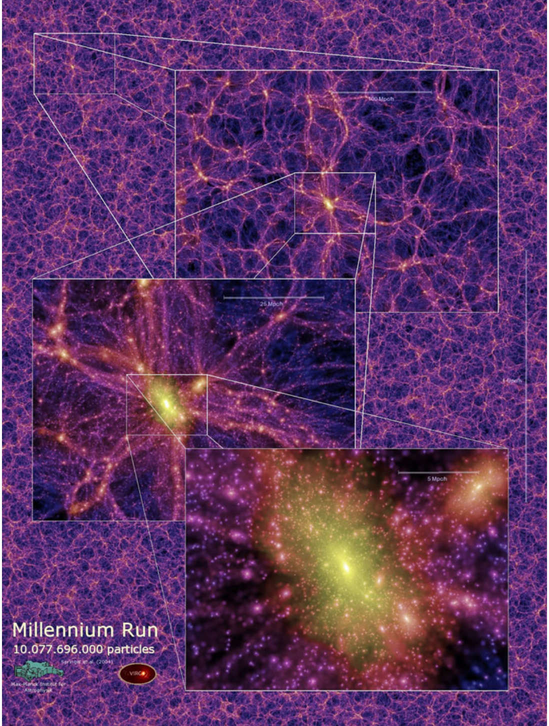
100 Mpc/h
25 Mpc/h
5 Mpc/h
Millennium Run
10.077.696.000 particles
Springel et al. (2004)
Max-Planck Institut für
Astrophysik

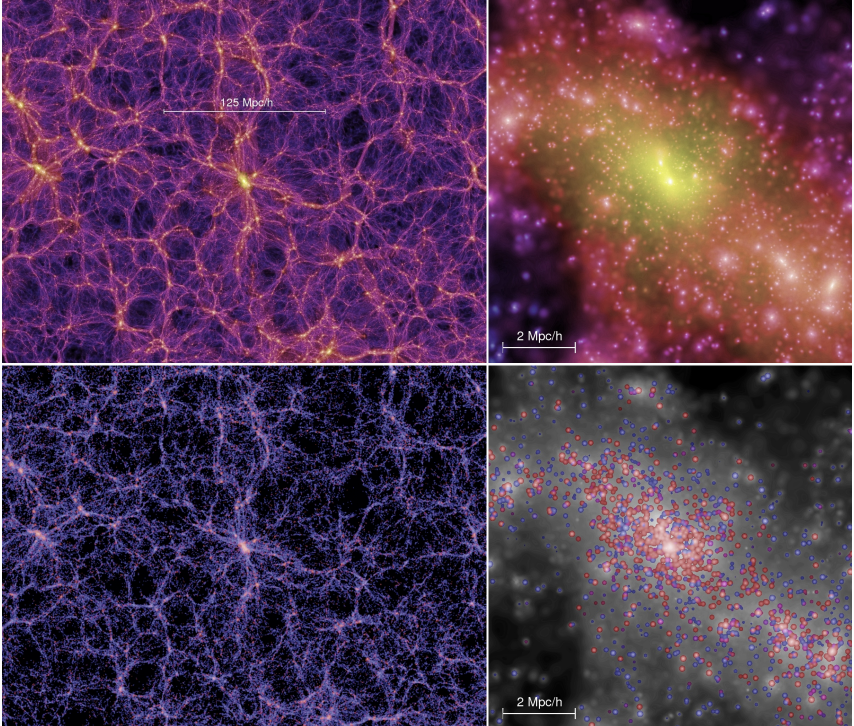
125 Mpc/h
2 Mpc/h
2 Mpc/h